Desert Dust Optical Properties from AERONET Observations: Spectral Absorption, Size Distributions, Spectral AOD and Seasonal Dynamics

Thomas F. Eck[1,2], Jeffrey S. Reid[3], Pawan Gupta[2], Elena Lind[2], Alexander Sinyuk[4,2], Antti Arola[5], Ilya Slutsker[4,2], Brent N. Holben[2], Joel S. Schafer[4,2], Mikhail G. Sorokin[4,2], Alexander Smirnov[4,2], Jason Kraft[6,2], Elizabeth A. Reid[3], Norman T. O'Neill[7]

(1) University of Maryland Baltimore County, Baltimore, MD, USA; (2) NASA/GSFC, Greenbelt, MD, USA; (3) US Naval Research Laboratory, Monterey, CA, USA; (4) Science Systems Applications, Inc., Lanham, MD, USA; (5) Finnish Meteorological Institute, Kuopio, Finland; (6) Fibertek Inc., Herndon, VA, USA (7) Centre d'Applications et de Recherches en Télédétection (CARTEL), Université de Sherbrooke, Sherbrooke, Quebec, Canada

Dust absorption – Iron Oxide Mineral content

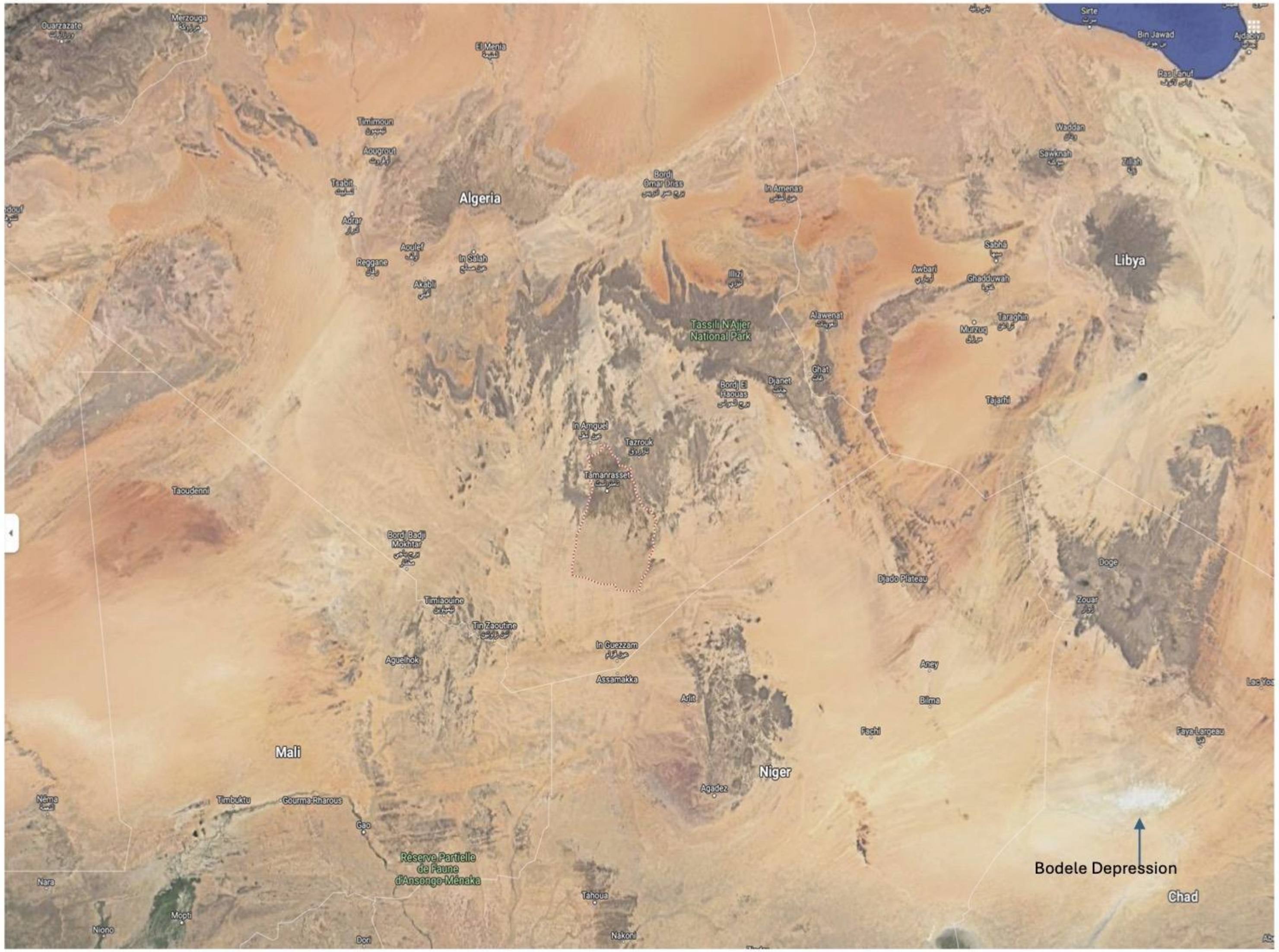

Satellite image of a portion of the Sahara and northern Sahel, showing the large variation in soil color. The Bodele Depression is nearly white (diatomaceous sediment) while some regions show redder color indicative of higher iron oxide content. Single Scattering Albedo (SSA) varies with Iron Oxide mass concentration.

Di Biagio et al. (2019) SSA vs. Iron Oxide

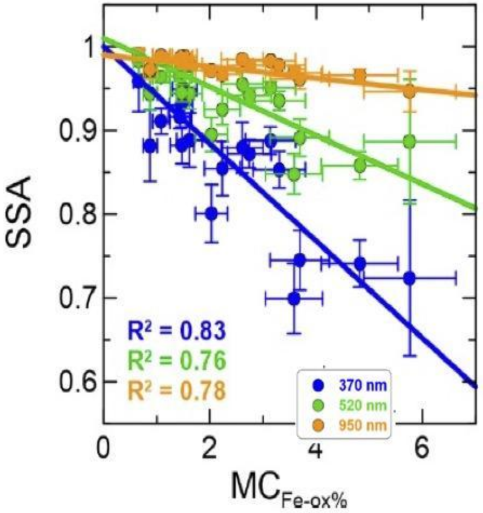

Di Biagio et al. (2019) ACP - Lab measurements of spectral SSA

Table 5. As in Table 4 for the single-scattering albedo (SSA) data. Mean, m

Sample	SSA						
region	0.37 µm	0.47 µm	0.52 µm	0.59 µm	0.66 µm	0.88 µm	0.95 µm
Tunisia	0.85	0.90	0.93	0.95	0.95	0.97	0.97
Morocco	0.92	0.95	0.96	0.98	0.98	0.98	0.99
Libya	0.89	0.93	0.95	0.98	0.98	0.98	0.98
Algeria	0.87	0.92	0.94	0.97	0.97	0.98	0.98
Mauritania	0.85	0.90	0.94	0.96	0.97	0.98	0.98
NAF–S	**0.88**	**0.92**	**0.94**	**0.97**	**0.97**	**0.98**	**0.98**
Niger	0.72	0.85	0.89	0.91	0.92	0.94	0.95
Mali	0.75	0.85	0.89	0.93	0.95	0.96	0.96
Bodélé	0.96	0.98	0.98	0.99	0.99	0.99	0.99
SAH	**0.81**	**0.89**	**0.92**	**0.94**	**0.95**	**0.96**	**0.97**
Ethiopia	0.80	0.86	0.90	0.92	0.94	0.97	0.97
Saudi Arabia	0.88	0.93	0.96	0.98	0.98	0.98	0.98
Kuwait	0.95	0.97	0.98	0.98	0.99	0.99	0.99
EAF–ME	**0.88**	**0.92**	**0.94**	**0.96**	**0.97**	**0.98**	**0.98**
Gobi	0.88	0.92	0.94	0.96	0.97	0.97	0.97
Taklimakan	0.82	0.88	0.92	0.95	0.96	0.96	0.96
EA	**0.85**	**0.90**	**0.93**	**0.96**	**0.96**	**0.97**	**0.97**
Arizona	0.93	0.96	0.97	0.98	0.98	0.99	0.99
NAM	**0.93**	**0.96**	**0.97**	**0.98**	**0.98**	**0.99**	**0.99**
Atacama	0.89	0.93	0.94	0.97	0.97	0.98	0.98
Patagonia	0.88	0.91	0.94	0.96	0.97	0.98	0.98
SAM	**0.89**	**0.92**	**0.94**	**0.96**	**0.97**	**0.98**	**0.98**
Namib-1	0.91	0.95	0.96	0.98	0.98	0.99	0.99
Namib-2	0.74	0.82	0.86	0.92	0.94	0.96	0.97
SAF	**0.83**	**0.88**	**0.91**	**0.95**	**0.96**	**0.98**	**0.98**
Australia	0.70	0.81	0.85	0.91	0.93	0.96	0.97
AUS	**0.70**	**0.81**	**0.85**	**0.91**	**0.93**	**0.96**	**0.97**
Mean	**0.85**	**0.91**	**0.93**	**0.96**	**0.96**	**0.97**	**0.98**
Median	**0.88**	**0.92**	**0.94**	**0.96**	**0.97**	**0.98**	**0.98**
10 %	**0.74**	**0.84**	**0.88**	**0.92**	**0.94**	**0.96**	**0.96**
90 %	**0.93**	**0.96**	**0.97**	**0.98**	**0.99**	**0.99**	**0.99**

Atmos. Chem. Phys., 19, 15503–15531, 2019
https://doi.org/10.5194/acp-19-15503-2019

Atmospheric Chemistry and Physics

Complex refractive indices and single-scattering albedo of global dust aerosols in the shortwave spectrum and relationship to size and iron content

Claudia Di Biagio[1], Paola Formenti[1], Yves Balkanski[2], Lorenzo Caponi[1,3], Mathieu Cazaunau[1], Edouard Pangui[1], Emilie Journet[1], Sophie Nowak[4], Meinrat O. Andreae[5,6], Konrad Kandler[7], Thuraya Saeed[8], Stuart Piketh[9], David Seibert[10], Earle Williams[11], and Jean-François Doussin[1]

Soil samples from various desert regions were re-suspended in a laboratory smog chamber and the scattering and absorption coefficients measured. These are therefore direct measurements of spectral SSA from 370 nm to 950 nm.

Comparisons of SSA from AERONET Retrievals to Laboratory Soil Sample Measurements

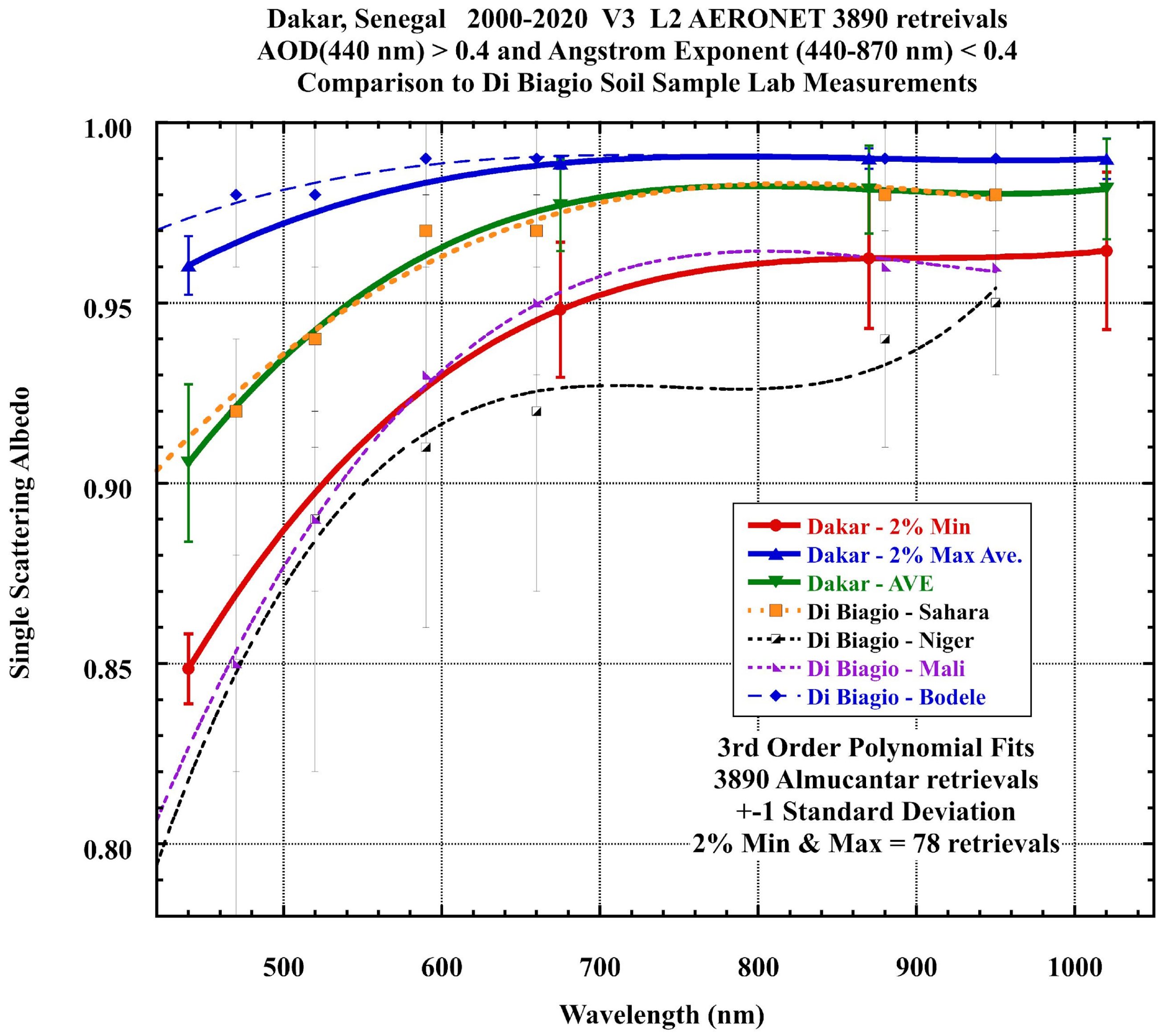

Climatological AERONET data of spectral SSA from > 20 year interval at Dakar, Senegal utilizing 3890 Level 2 retrievals

AOD(440) > 0.4 = L2 criteria for uncertainty in SSA of <=0.03

Angstrom Exponent < 0.4 = Dust dominated cases

2% minimum and maximum SSA populations from AERONET represent the 2 standard deviation tails

Note the tight agreement between the AERONET climatological average SSA and the Sahara average from Di Biagio (2019)

Western Atlantic

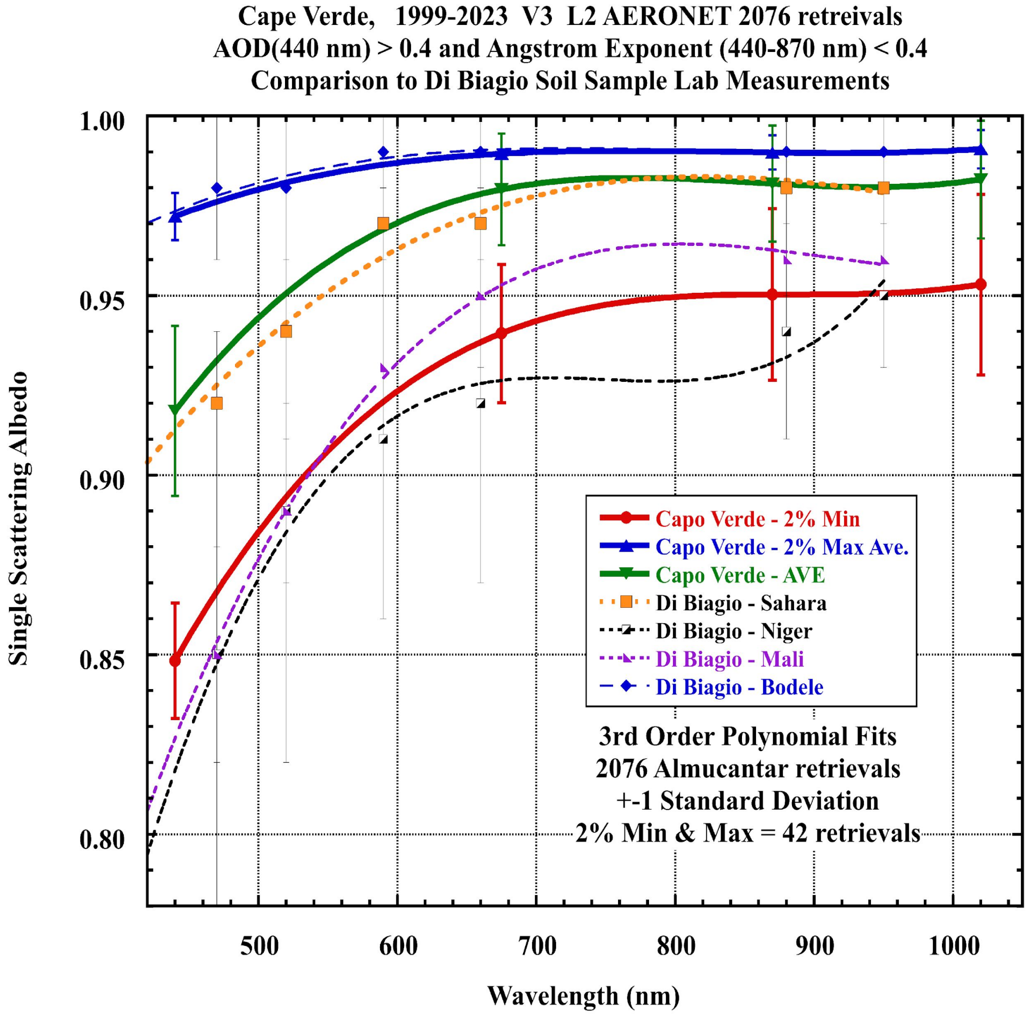

Eastern Atlantic – Trans-oceanic transport

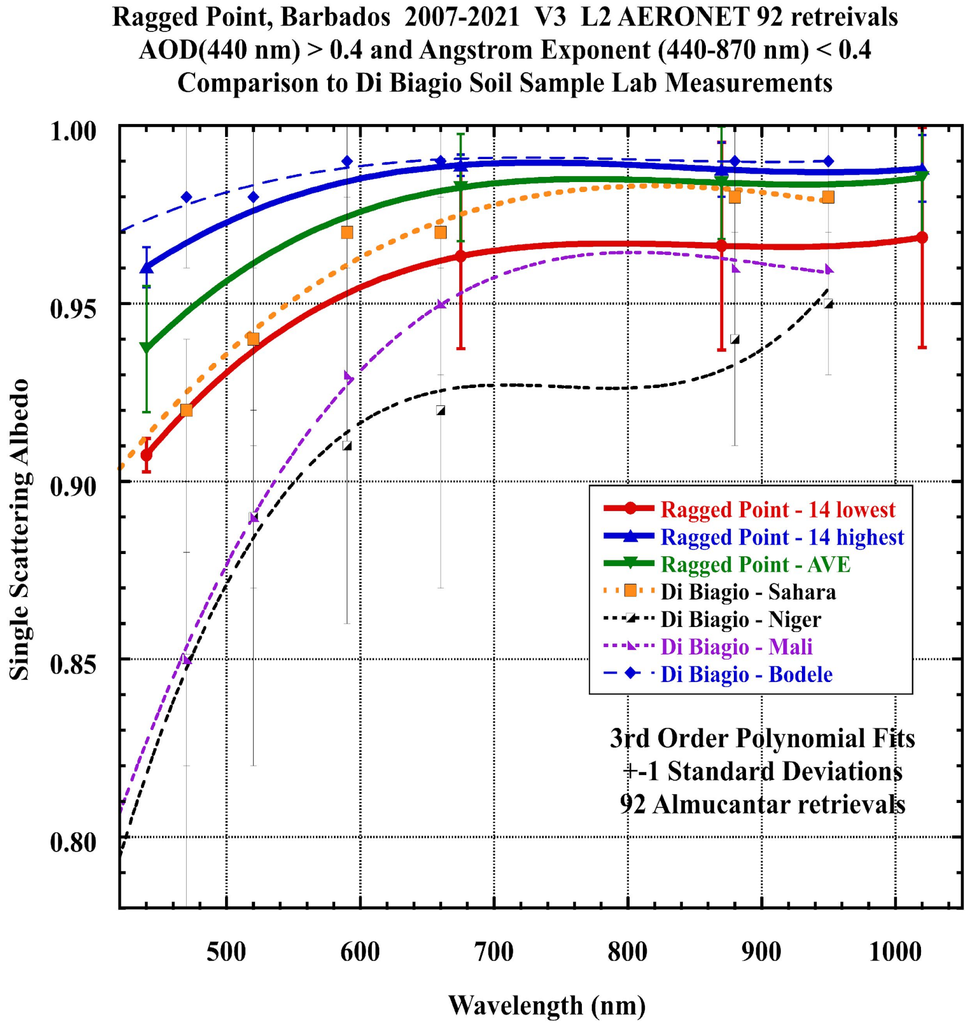

Ave. SSA and minimum SSA at Ragged Point, Barbados are significantly higher as compared to Cape Verde.

Possible factors:
(1) Maybe dust sources for largest trans-Atlantic transport events have higher SSA

(2) possible size distribution changes in trans-Atlantic transport

(3) Small sample size at Barbados (92) may not be truly representative versus robust sample at Cape Verde (2076).

Note: Ragged Point, Barbados only has 92 total L2 Almucantars with AOD(440)>0.4 and AE<0.4 due to combination of plume spreading and dilution plus wet + dry deposition after crossing the Atlantic Ocean
Only ~1 standard deviation tails shown since 2 sigma would be too few observations

Saudi Arabia

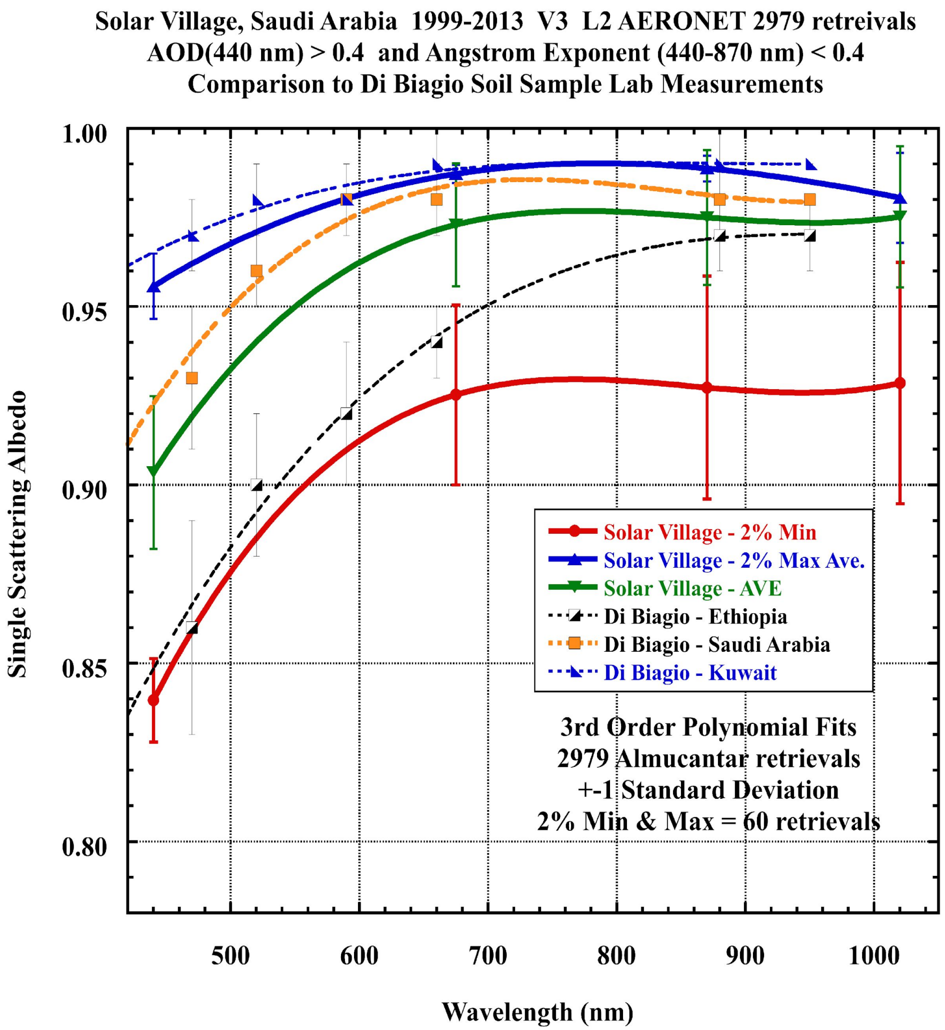

Australia

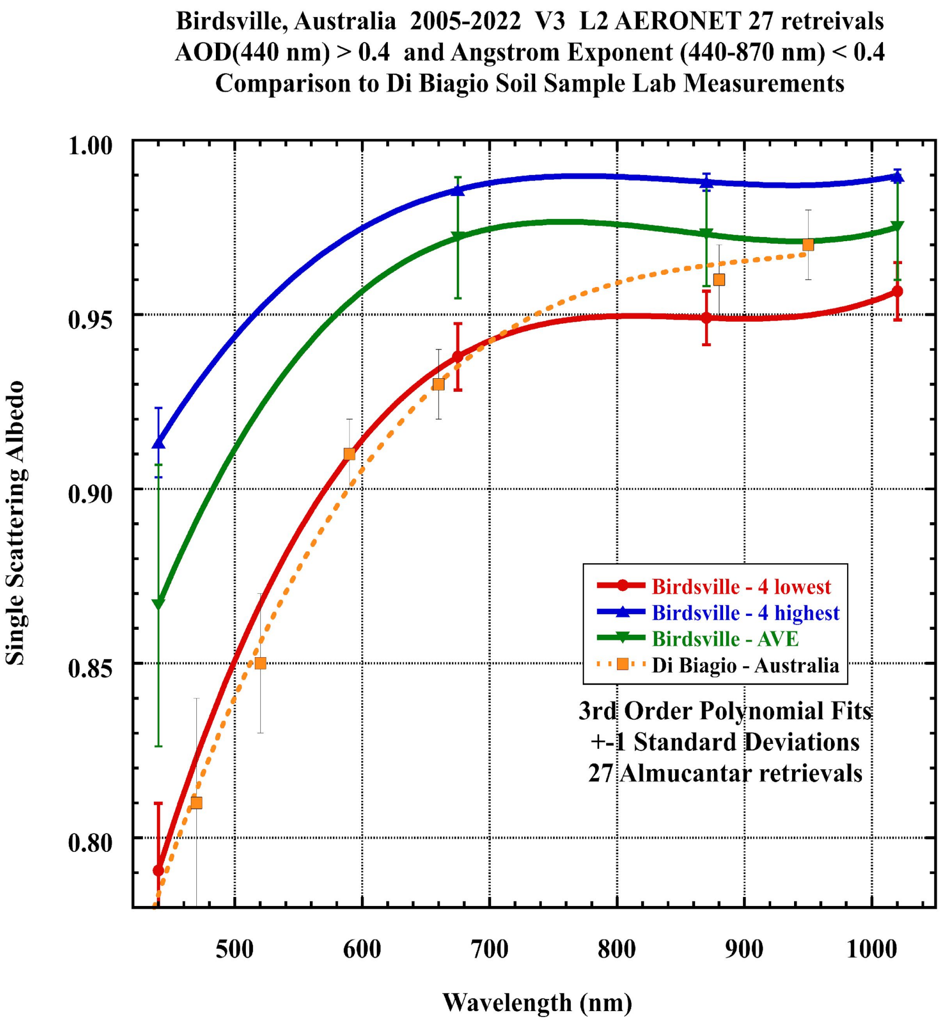

Note: Birdsville, Australia only has 27 total L2 Almucantars with AOD(440)>0.4 and AE<0.4
Note that for Birdsville the **lowest** SSA retrievals agree closely with the Di Biagio measurements

Birdsville, Australia

Large variability in soil color in the vicinity of Birdsville, Australia.
More red color is indicative of high iron oxide content while tan and brown soils indicate lower iron oxide content.
Airborne soil dust at Birdsville would therefore be expected to have significant variation in absorption magnitude in short wavelengths.

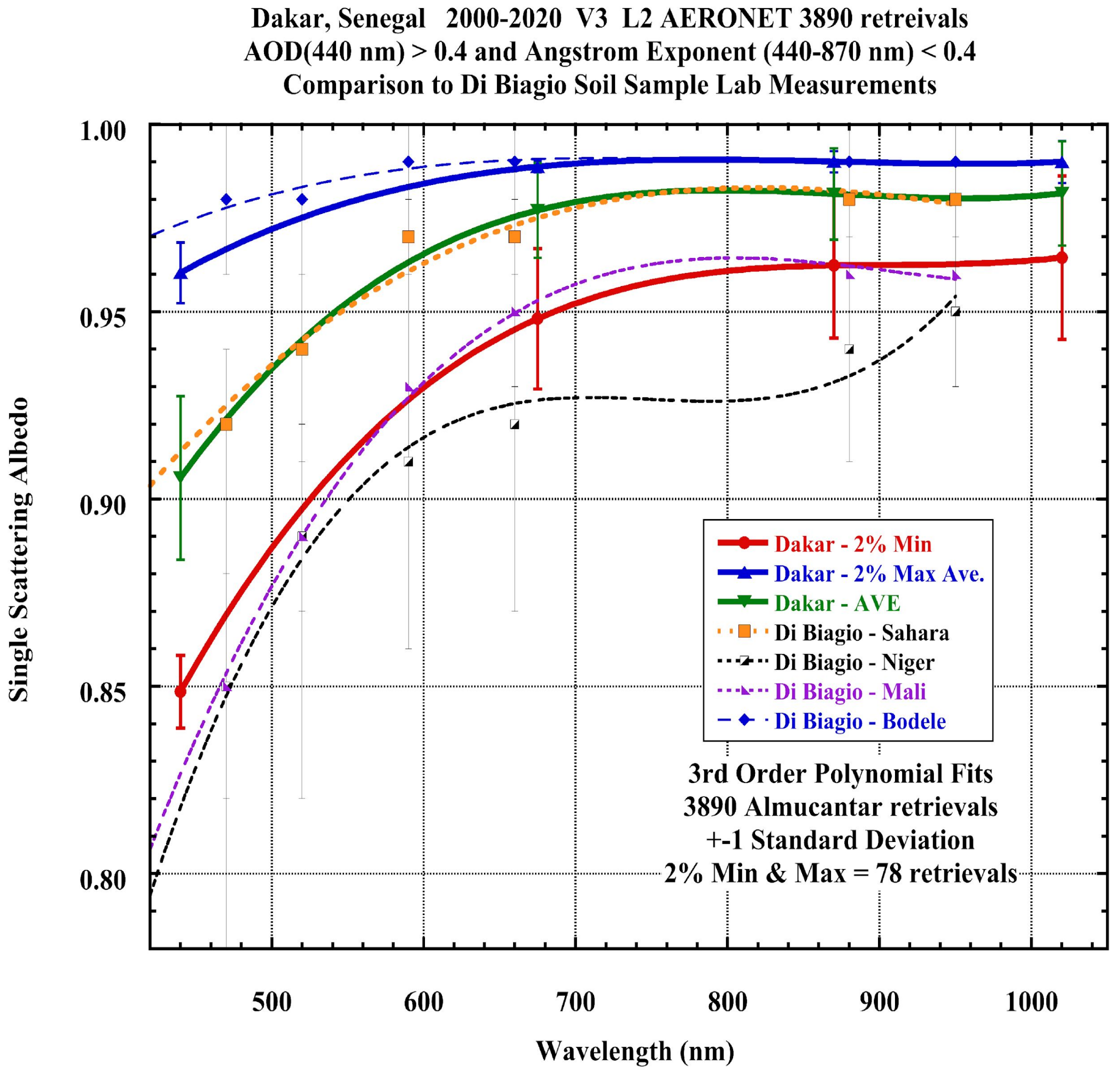

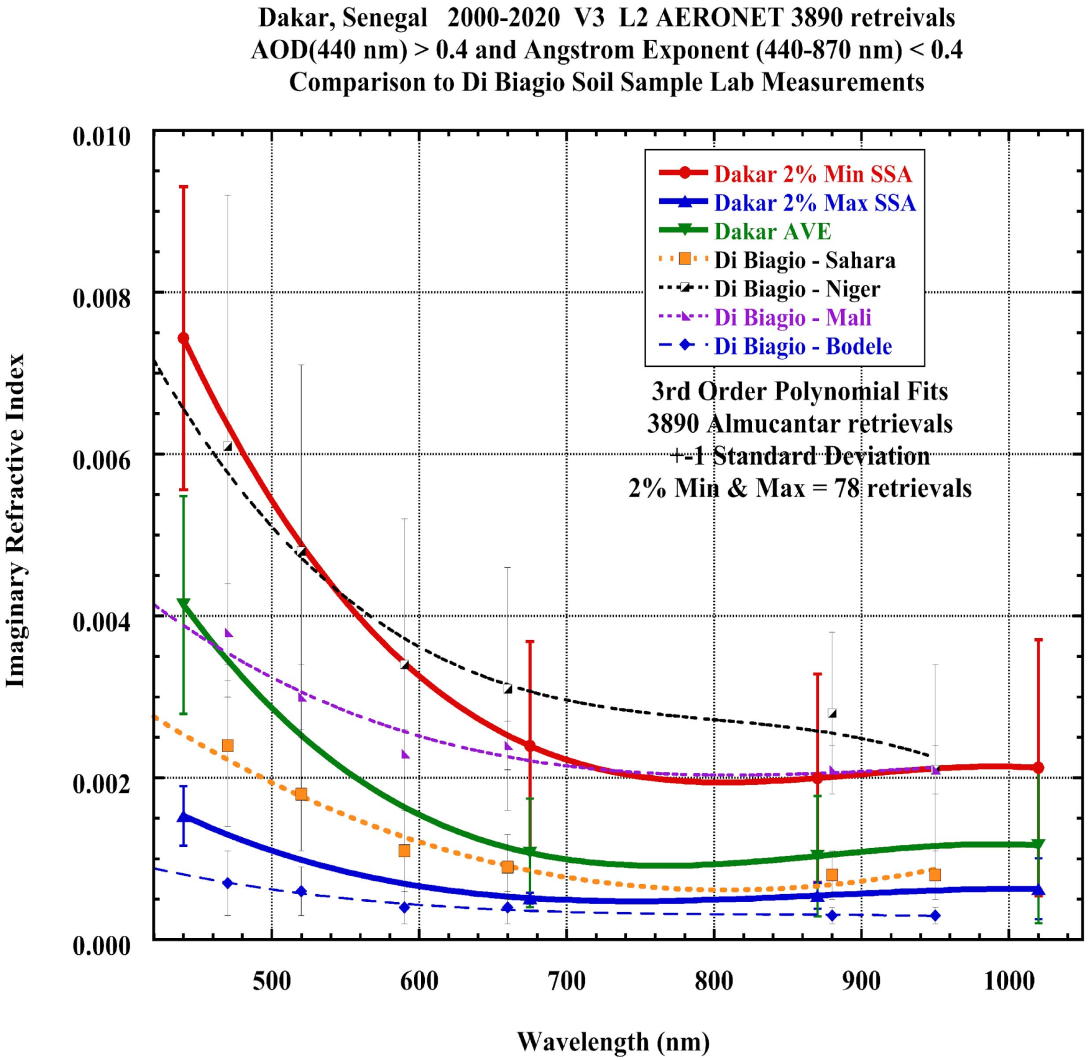

While the SSA of Di Biagio (2019) are computed from directly from scattering and absorption coefficient measurements, the imaginary refractive index is computed by them from Mie code using the measured size distributions and optical data. Therefore the dust is (erroneously) assumed to be spherical and this introduces some uncertainty in calculated refractive indices.

Climatological multi-year averages of SSA and Aerosol Size Distributions

Birdsville, Australia is significantly more absorbing while Ragged Point, Barbados is the least absorbing.

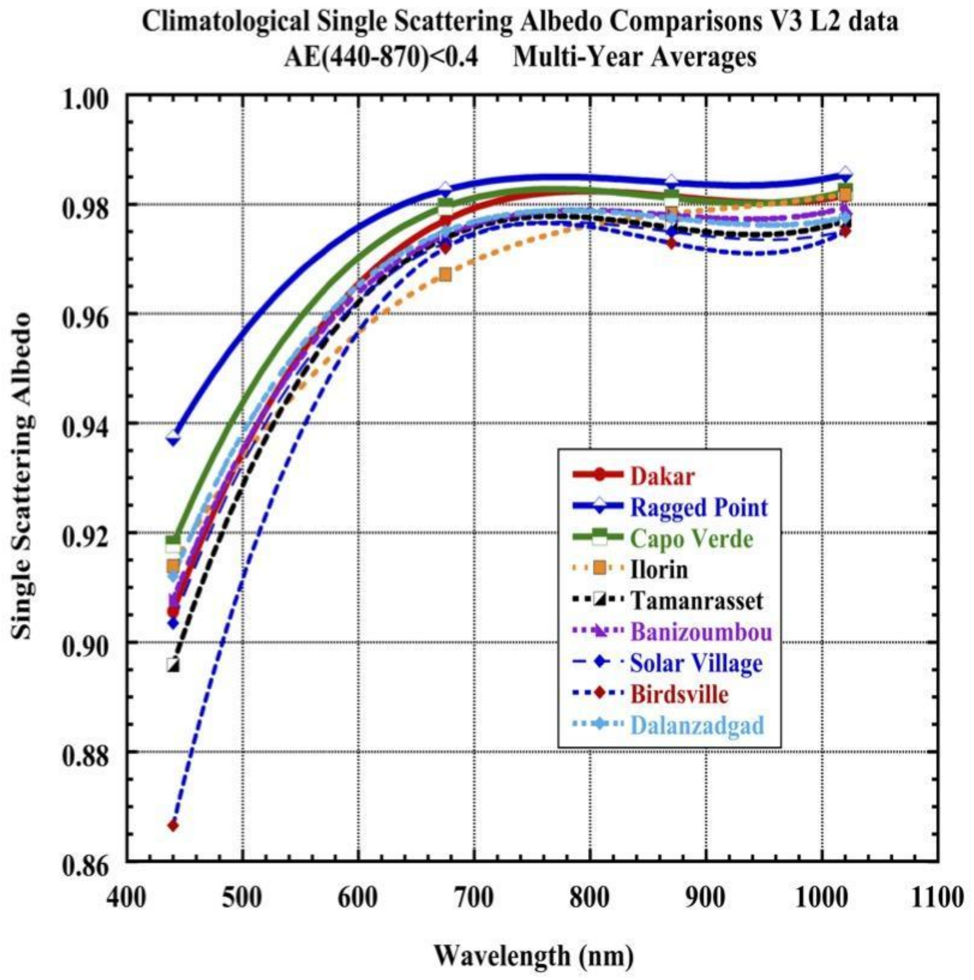

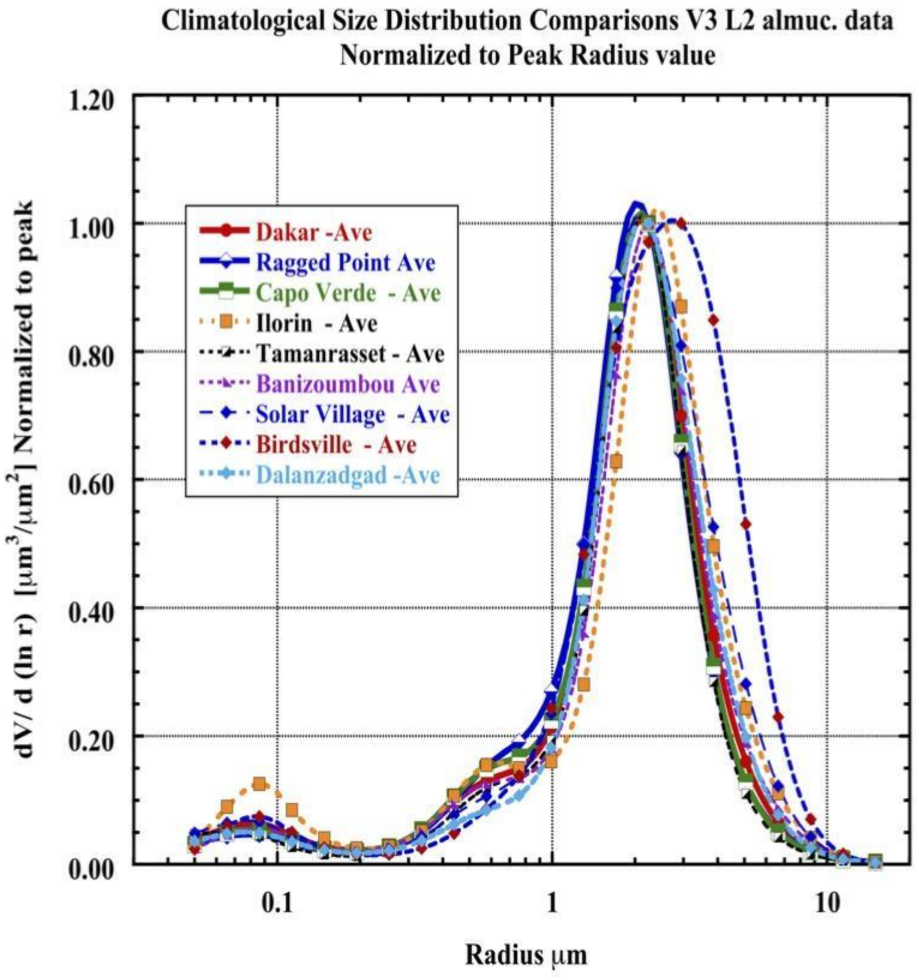

Spectral Imaginary Refractive index shows significant spread at 440 nm while more uniformly low at longer wavelengths.

Spectral Real Refractive index is similar for all Saharan/Sahelian dust sites but consistently higher for all other desert site regions

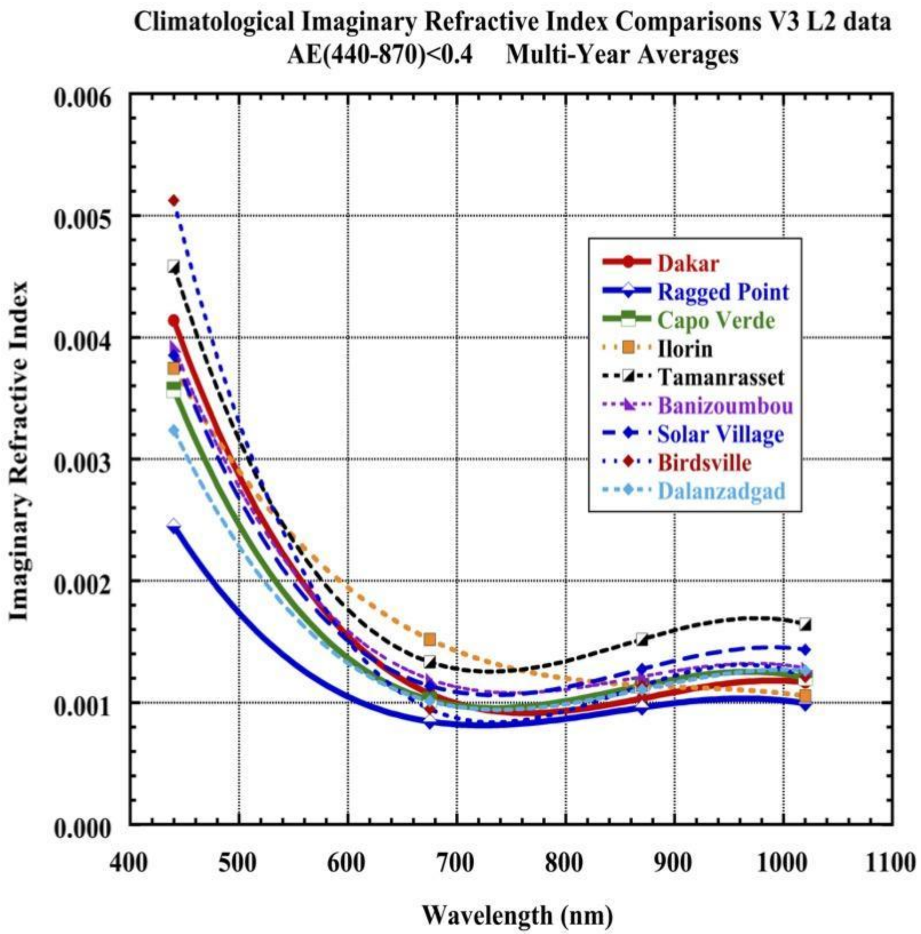

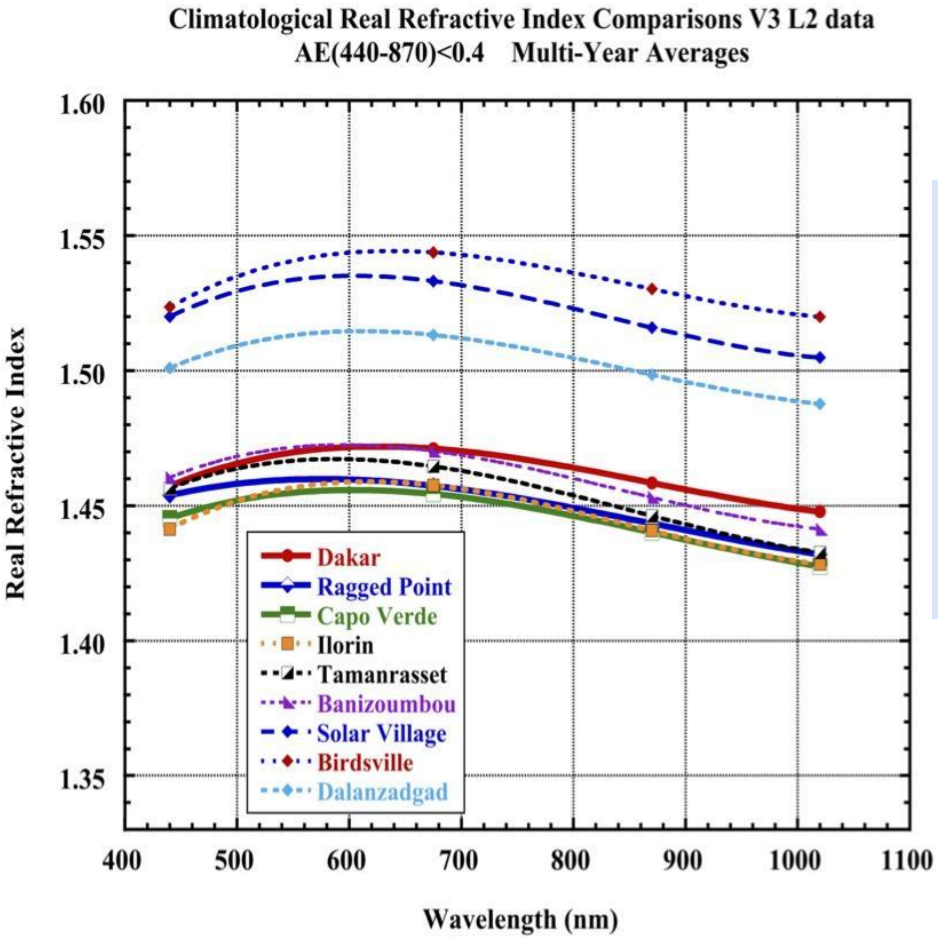

Di Biagio et al. (2019)
Real Part RI
Sahara & Sahel range
1.49-1.52
Middle East & East Africa
1.50-1.55
Australia
1.54
Asia (Gobi & Taklamakan)
1.48 & 1.54

Temporal Variability of SSA at Ilorin, Nigeria - 4 Ch. & 6 Ch. Retrievals

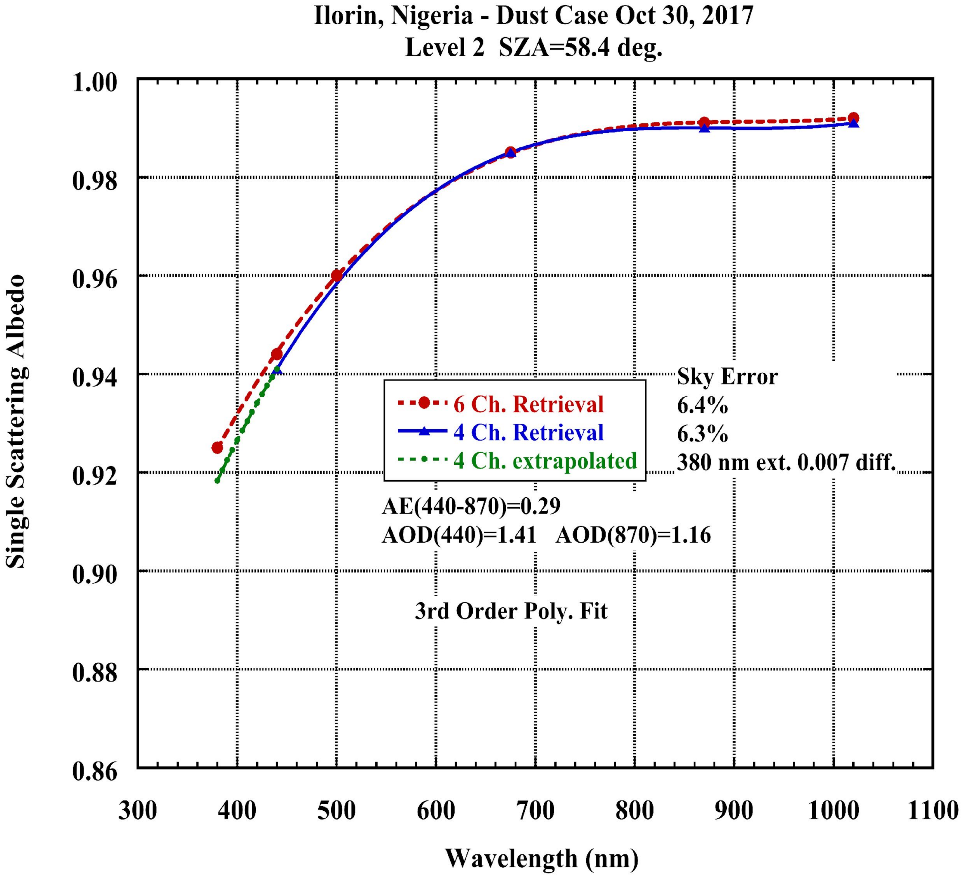

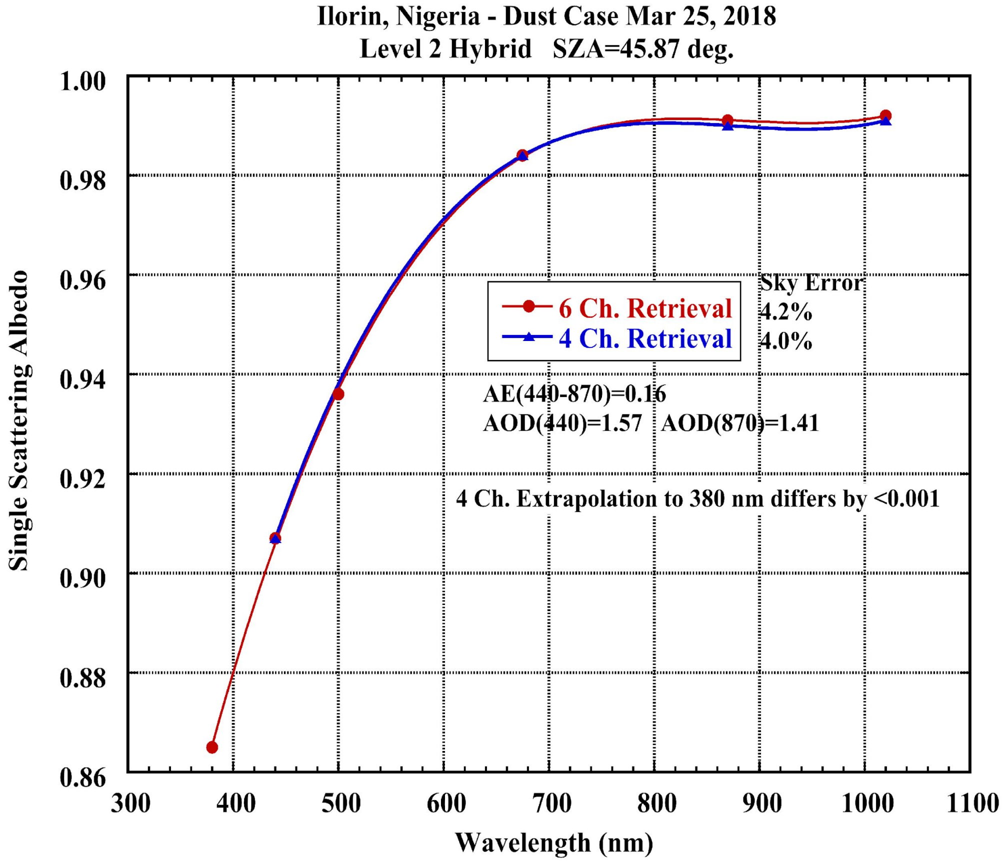

A 3rd order Polynomial fit is excellent for all wavelengths in the range of 380 to 1020 nm. The 6-channel retrieval is nearly identical to the 4-channel retrieval except for extending to 380 nm. This suggests that <u>for dust SSA</u> the 4 channel retrievals of old Cimels that lack the 380 nm sky radiances the SSA can be reliably extrapolated to 380 nm.

Back trajectories to the Ilorin, Nigeria site

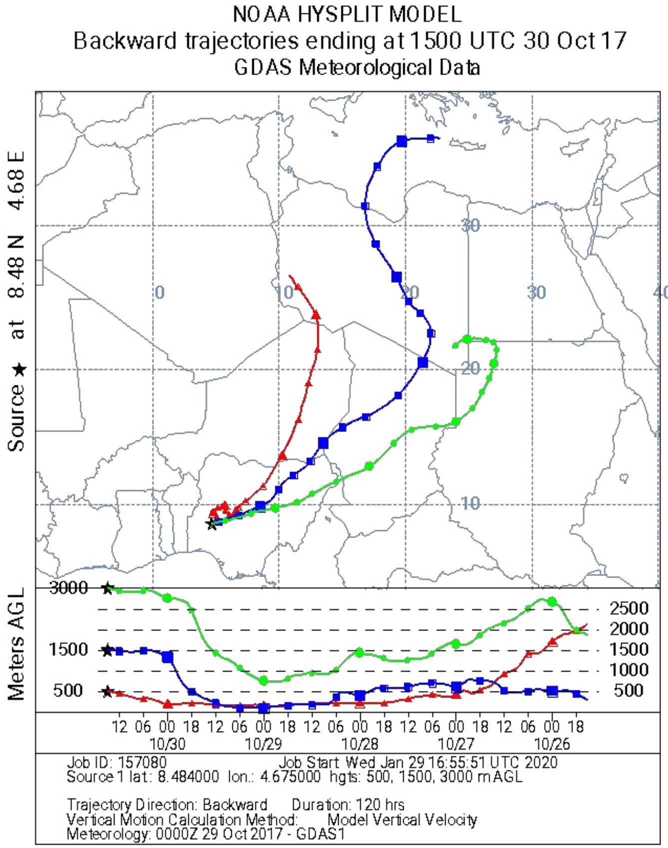

Oct. 30, 2017 trajectory in blue passes directly over the Bodele Depression which is a source of very weakly absorbing diatomite sediments.
Mar 25, 2018 trajectory in blue passes over a different region of the Sahara, not even close to the Bodele Depression.

The higher SSA in the Oct 30, 2017 retrievals is consistent with the characteristics of the mineral source in the Bodele Depression

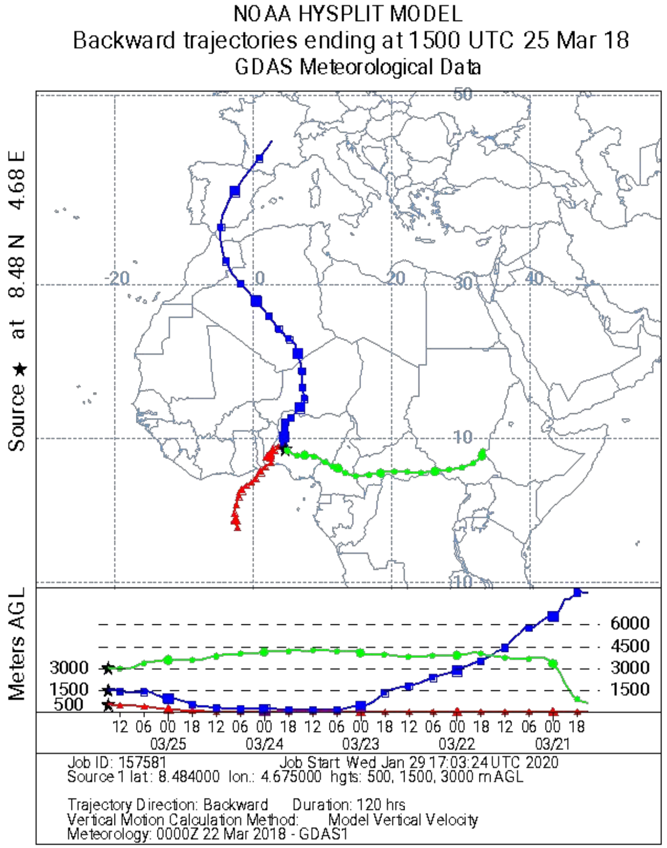

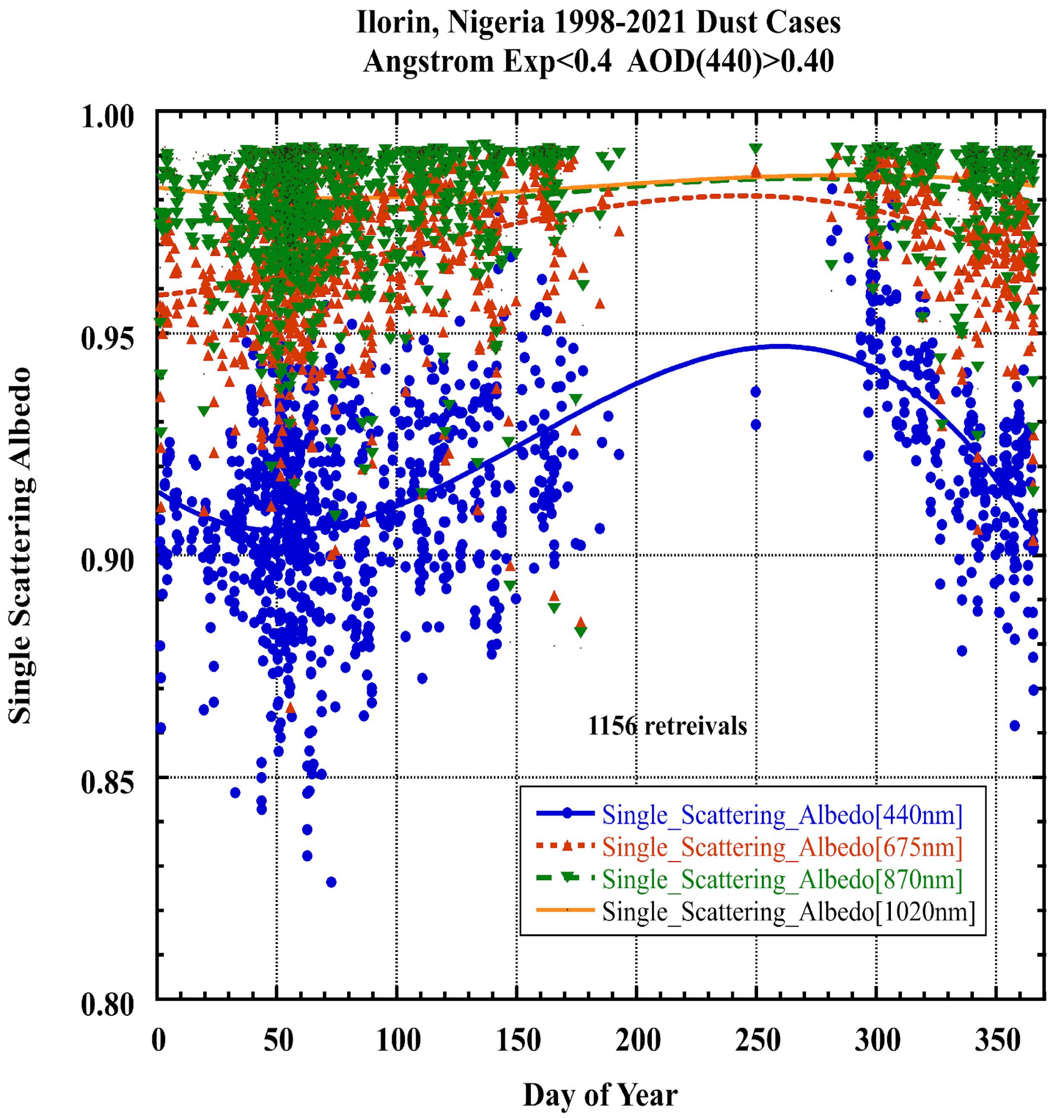

Ilorin, Nigeria 1998-2021 Dust Cases
Angstrom Exp<0.4 AOD(440)>0.40
Single Scattering Albedo
Day of Year
1156 retreivals
Single_Scattering_Albedo[440nm]
Single_Scattering_Albedo[675nm]
Single_Scattering_Albedo[870nm]
Single_Scattering_Albedo[1020nm]

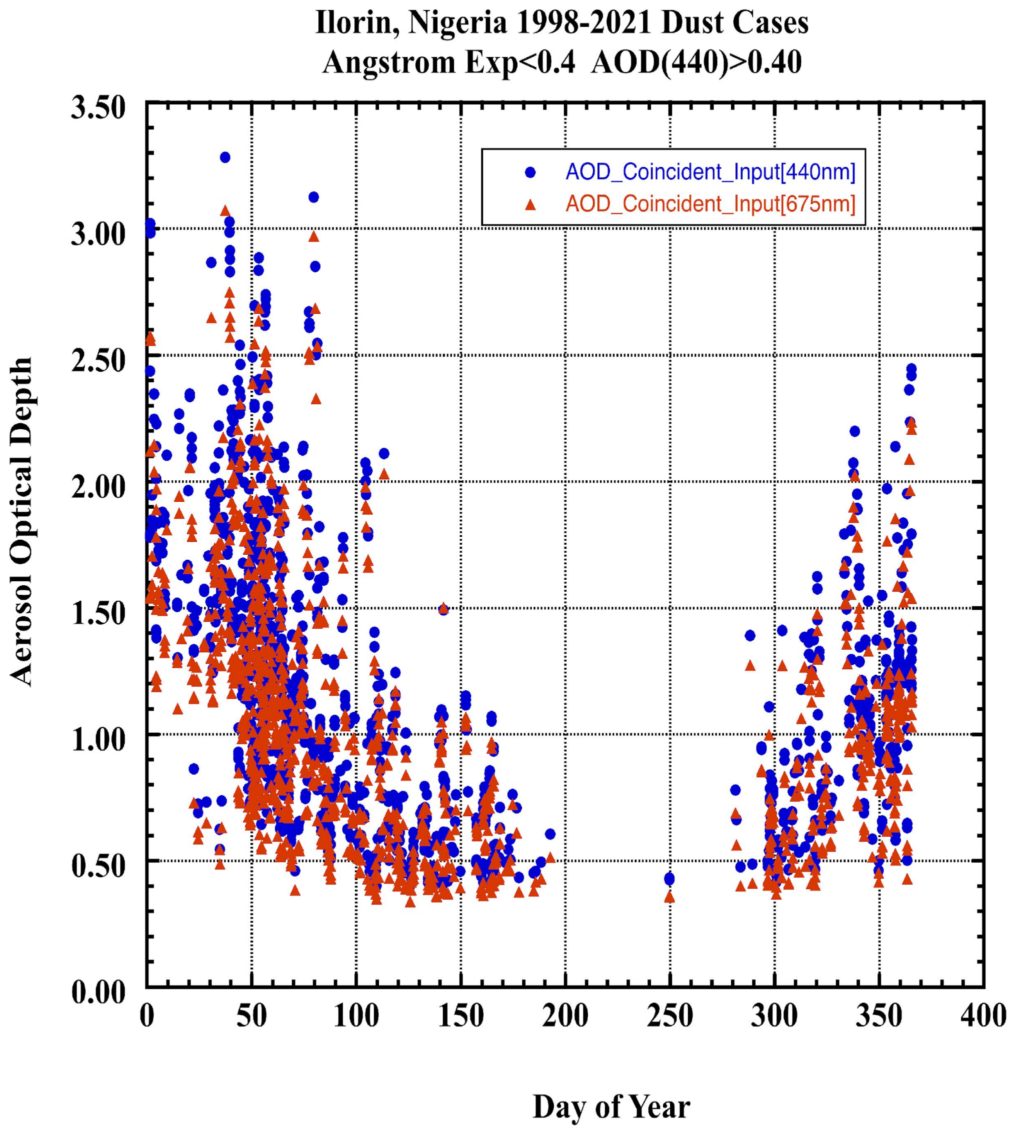

Ilorin, Nigeria 1998-2021 Dust Cases
Angstrom Exp<0.4 AOD(440)>0.40
Aerosol Optical Depth
Day of Year
AOD_Coincident_Input[440nm]
AOD_Coincident_Input[675nm]

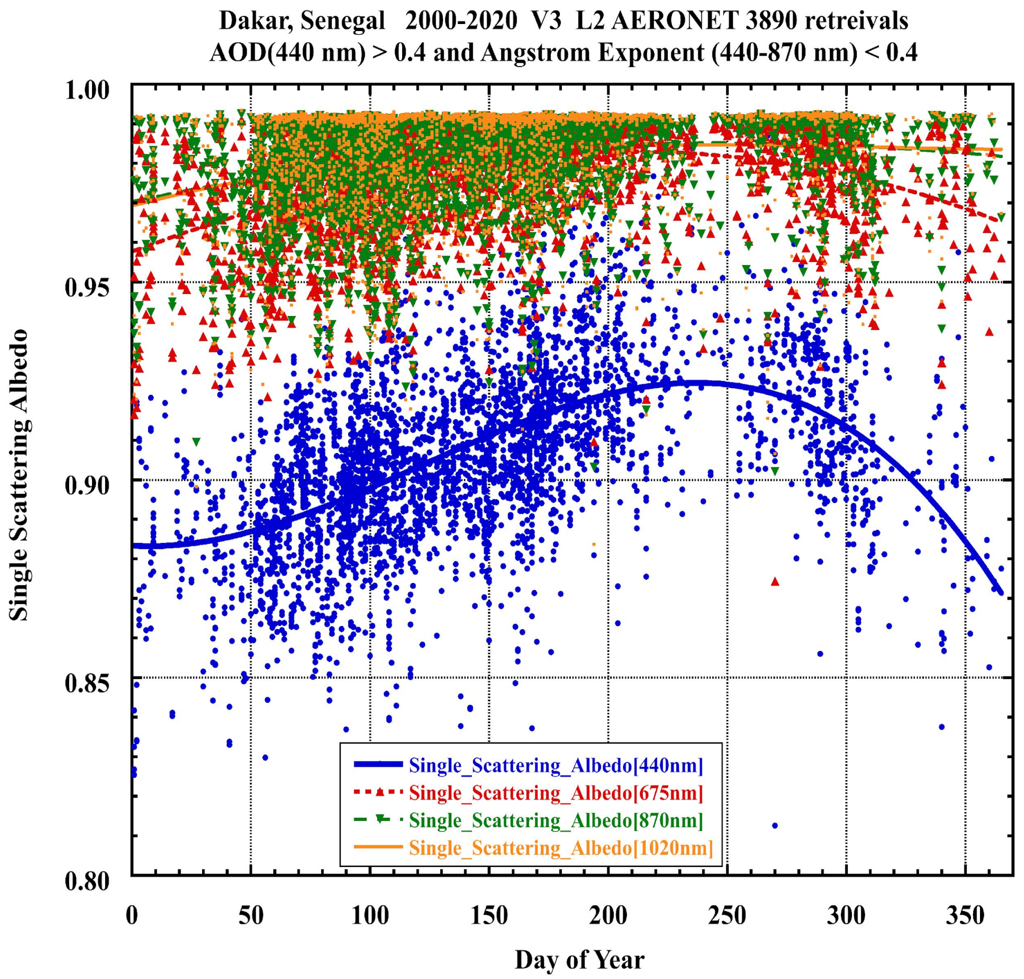
Dakar, Senegal 2000-2020 V3 L2 AERONET 3890 retreivals
AOD(440 nm) > 0.4 and Angstrom Exponent (440-870 nm) < 0.4
Single Scattering Albedo
Day of Year
Single_Scattering_Albedo[440nm]
Single_Scattering_Albedo[675nm]
Single_Scattering_Albedo[870nm]
Single_Scattering_Albedo[1020nm]

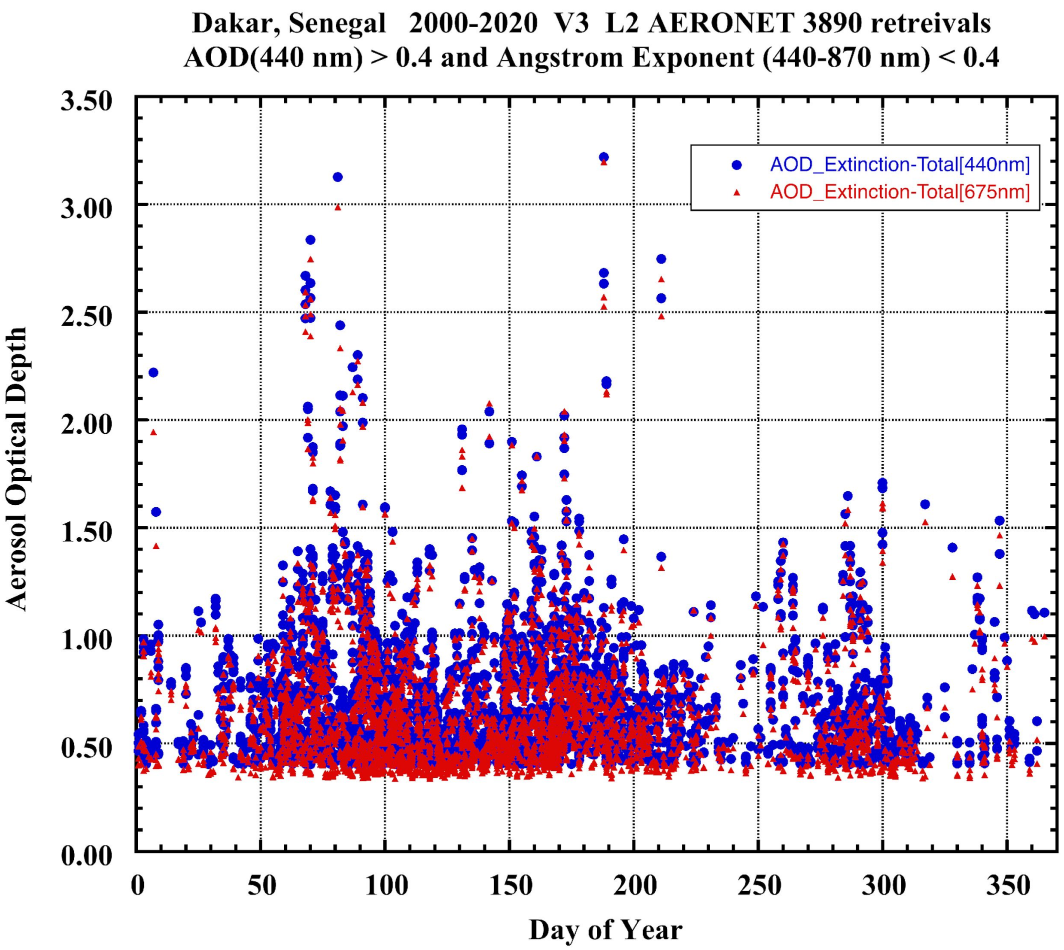
Dakar, Senegal 2000-2020 V3 L2 AERONET 3890 retreivals
AOD(440 nm) > 0.4 and Angstrom Exponent (440-870 nm) < 0.4
Aerosol Optical Depth
Day of Year
AOD_Extinction-Total[440nm]
AOD_Extinction-Total[675nm]

Sahara/Sahel Size distributions

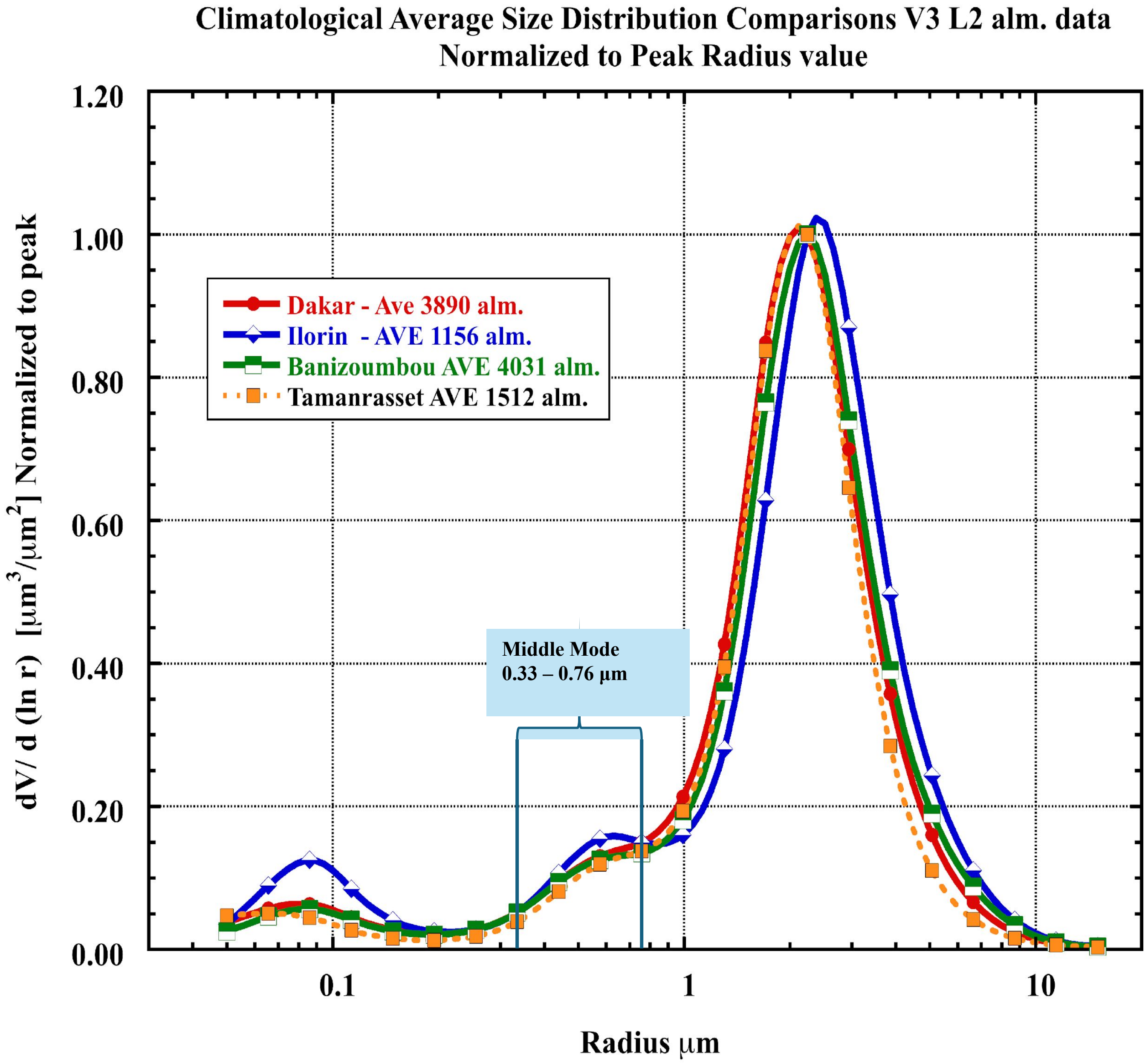

The 'middle mode' sized particles (volume radius 0.33 - 0.76 µm) are present in site averages of AERONET retrievals for all sites in the Sahara and Sahel, when AOD(440)>0.4 and AE(440-870)<0.4.
This persistent mode results in a large fine mode fraction of aerosol optical depth (~40% at 440 nm; if fine mode is defined as radius<0.76 µm) for the majority of dust events from the world's largest sources of airborne soil dust.

Additionally, this middle mode of <u>diameters</u> 0.66 to 1.52 µm is well within the PM2.5 size range of diameter <2.5 micron, therefore readily inhalable and a significant human health risk.

Quarterly Journal of the Royal Meteorological Society *Q. J. R. Meteorol. Soc.* (2011)

RMetS
Royal Meteorological Society

Comparison of in situ aircraft measured to AERONET retrievals of Dust Size Distributions

Physical and optical properties of mineral dust aerosol measured by aircraft during the GERBILS campaign

B. T. Johnson* and S. R. Osborne
Met Office, Exeter, UK

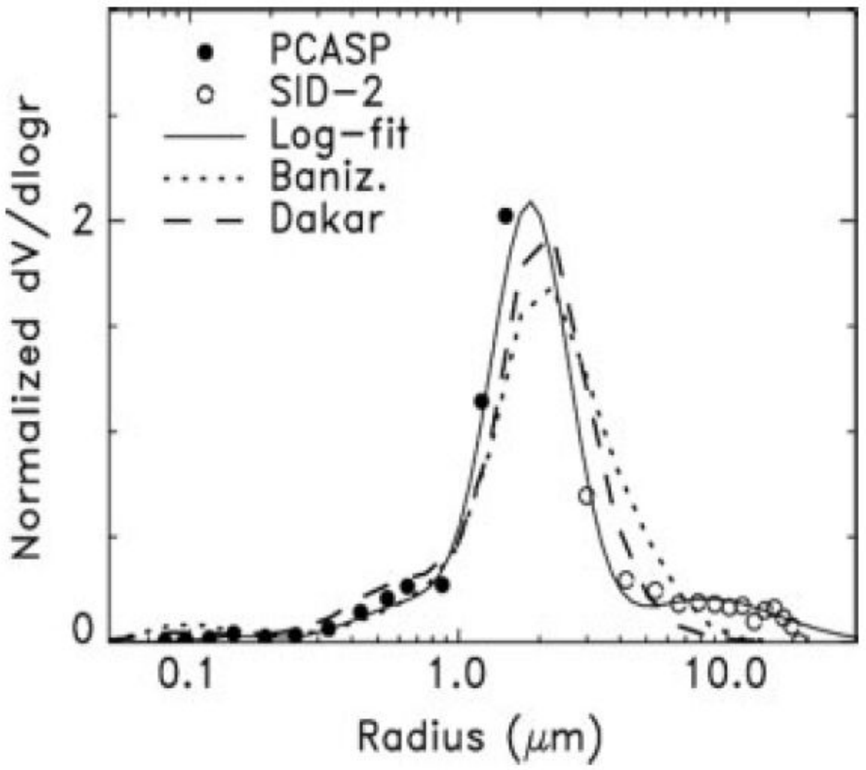

Figure 4. Campaign-mean volume distribution from the BAe-146 aircraft (PCASP and SID-2, plus log-normal fit) and from AERONET retrievals made at Banizoumbou and Dakar.

Middle mode sized dust particles were observed <u>from in situ aircraft sampling</u> during the GERBILS campaign in the western Sahara and Sahel in June 2007. These were campaign averaged size distributions from flights that transited thousands of kilometers over this dust source region.
These in situ campaign averaged size distributions agreed well with AERONET retrievals made at two sites within the aircraft sampled spatial domain. The AERONET size distributions are 12-day averages over the same time interval as the aircraft flights in late June 2007.

N.A. Drake, I. Candy, P. Breeze et al. **Ancient Mega-Lakes of the Sahara** Quaternary Science Reviews 276 (2022) 107318

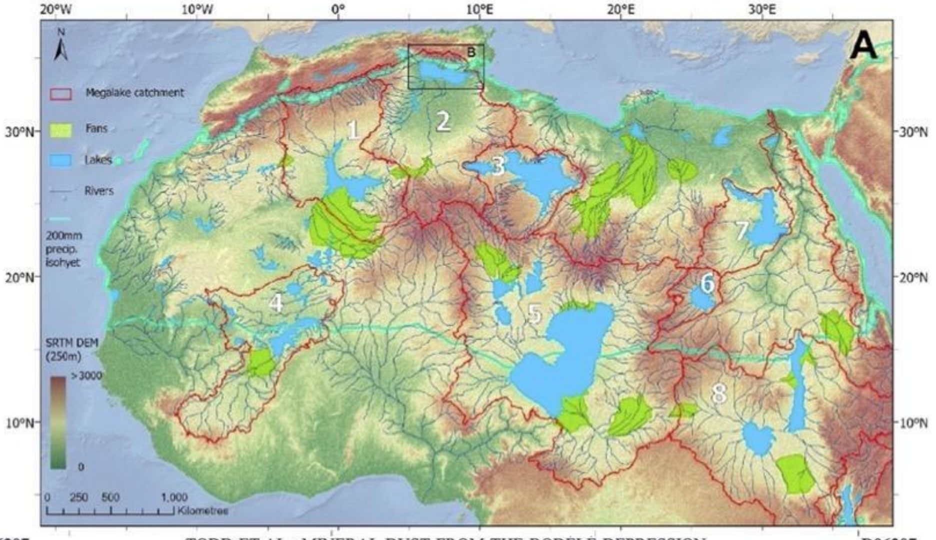

D06207 TODD ET AL.: MINERAL DUST FROM THE BODELE DEPRESSION D06207

Todd et al. (2007); JGR

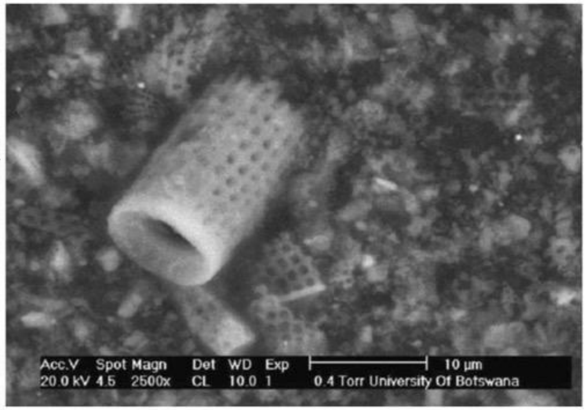

Figure 7. SEM image of dust sample collected on 10 March 2005 at the BoDEx field site. Clearly visible are crushed diatom fragments from the dry paleolake bed.

JOURNAL OF GEOPHYSICAL RESEARCH, VOL. 106, NO. D16, PAGES 18,20

Climatology of dust aerosol size distribution and optical properties derived from remotely sensed data in the solar spectrum

D. Tanré,[1] Y. J. Kaufman,[2] B. N. Holben,[3] B. Chatenet,[4] A. Karnieli,[5] F. Lavenu,[6] L. Blarel,[1] O. Dubovik,[7] L. A. Remer,[2] and A. Smirnov[7]

Tanré et al. (2001)

18,208 TANRE ET AL.: PHYSICAL AND OPTICAL

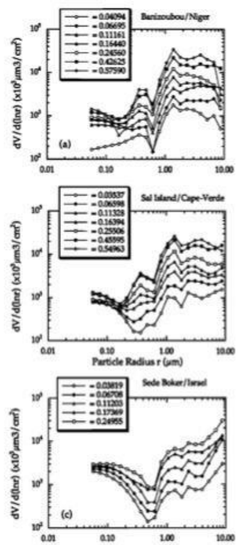

Figure 2. Volume size distribution derived from the sky radiances as a function of the particle radius. The distributions have been averaged over 10–15 individual size distributions and sorted according to the aerosol optical thickness measured at 1020 nm. (a) Banizoumbou, (b) Sal Island, (c) Sede Boker.

JOURNAL OF GEOPHYSICAL RESEARCH: ATMOSPHERES, VOL. 118, 12,661–12,672, doi:10.1002/2013JD020342, 2013

Evidence of a weakly absorbing intermediate mode of aerosols in AERONET data from Saharan and Sahelian sites

Scott M. Gianelli,[1,2,3] Andrew A. Lacis,[4] Barbara E. Carlson,[4] and Sultan Hameed[1]

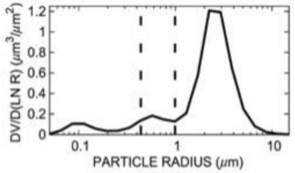

Figure 2. The mean values for the AERONET size distribution retrievals at the Ilorin site on 10 February 2000. The vertical dashed lines denote the values of the particle radius (0.439 µm and 0.992 µm) between which a peak in the retrieved size distribution must lie for the intermediate mode to be flagged.

Gianelli et al. (2013)

Sahara/Sahel - Middle Mode Dust: Consistent presence throughout the year

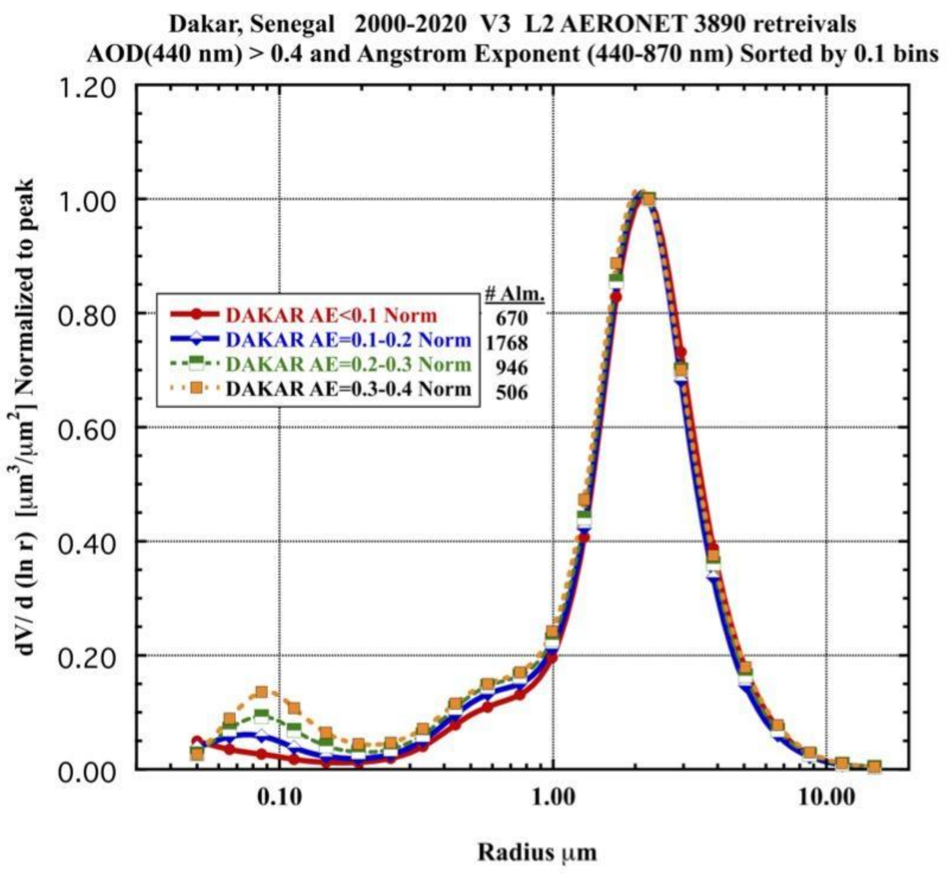

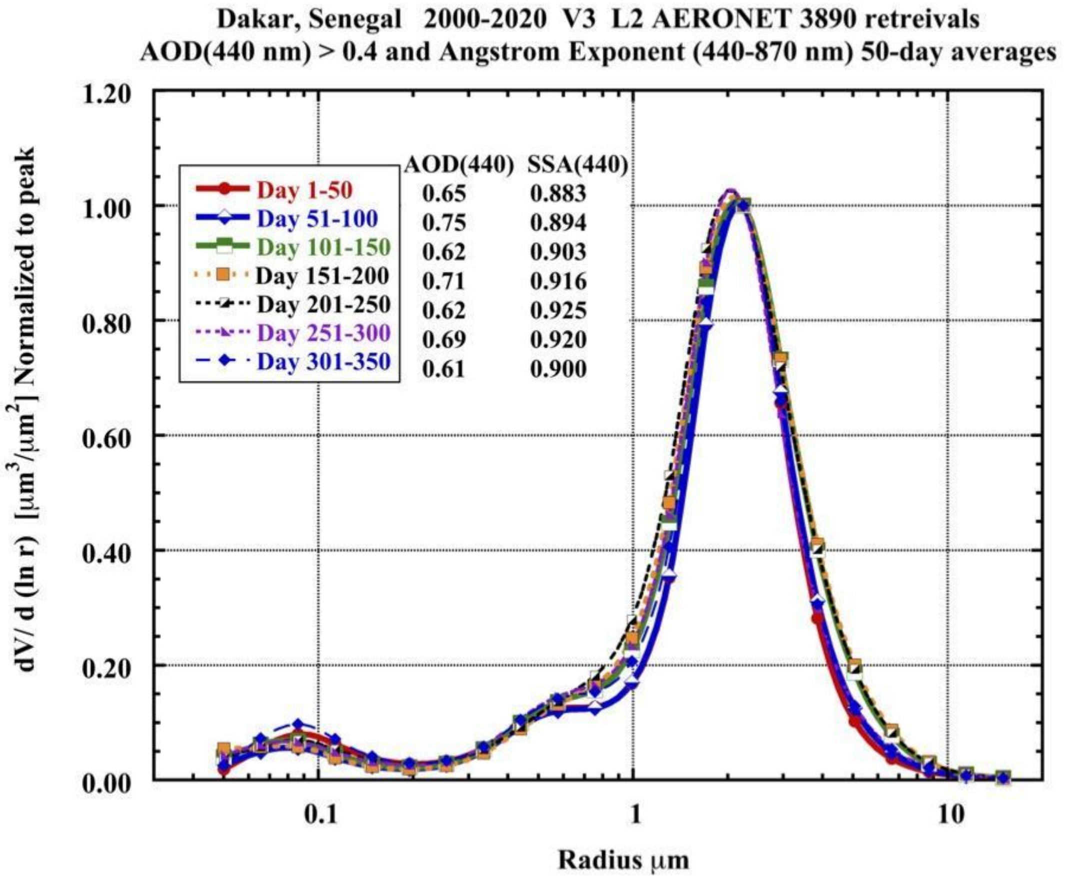

The coarse mode (radius >1 micron) is very similar for all ranges of Angstrom Exponent (440-870) < 0.4. The middle mode (0.33 – 0.76 μm radius) shows a small decrease for AE<0.1 while the other three AE ranges are similar. The fine mode (<0.33 μm) shows the largest variation as a function of AE range.

Note that middle mode (~0.33 – 0.76 micron radius) size particles are present throughout the year in relatively similar relative concentrations.

Dust case with AE(440-870)=0.193 However the Fine mode Fraction of AOD =0.47 at 440 nm

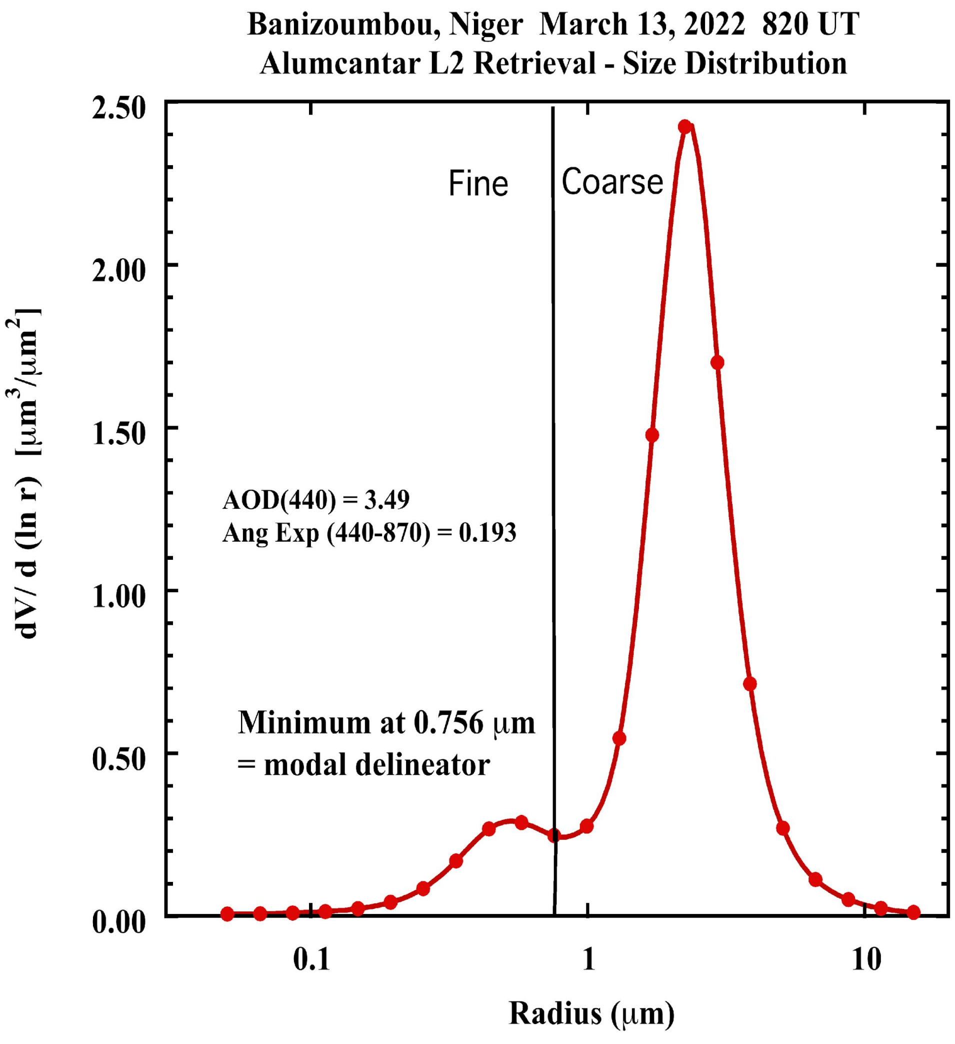

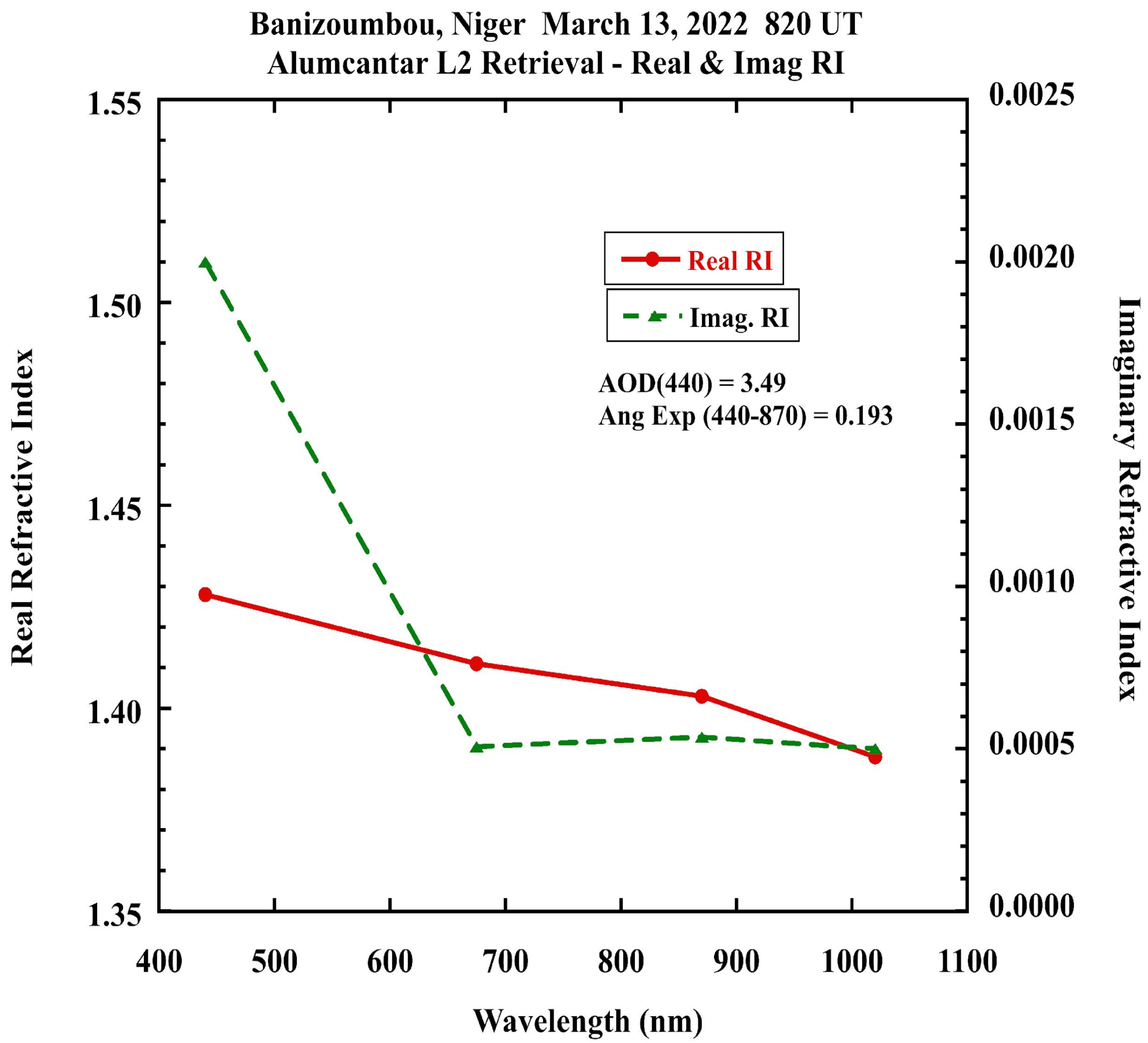

Dust case with AE(440-870)=0.193 However the Fine mode Fraction of AOD =0.47 at 440 nm

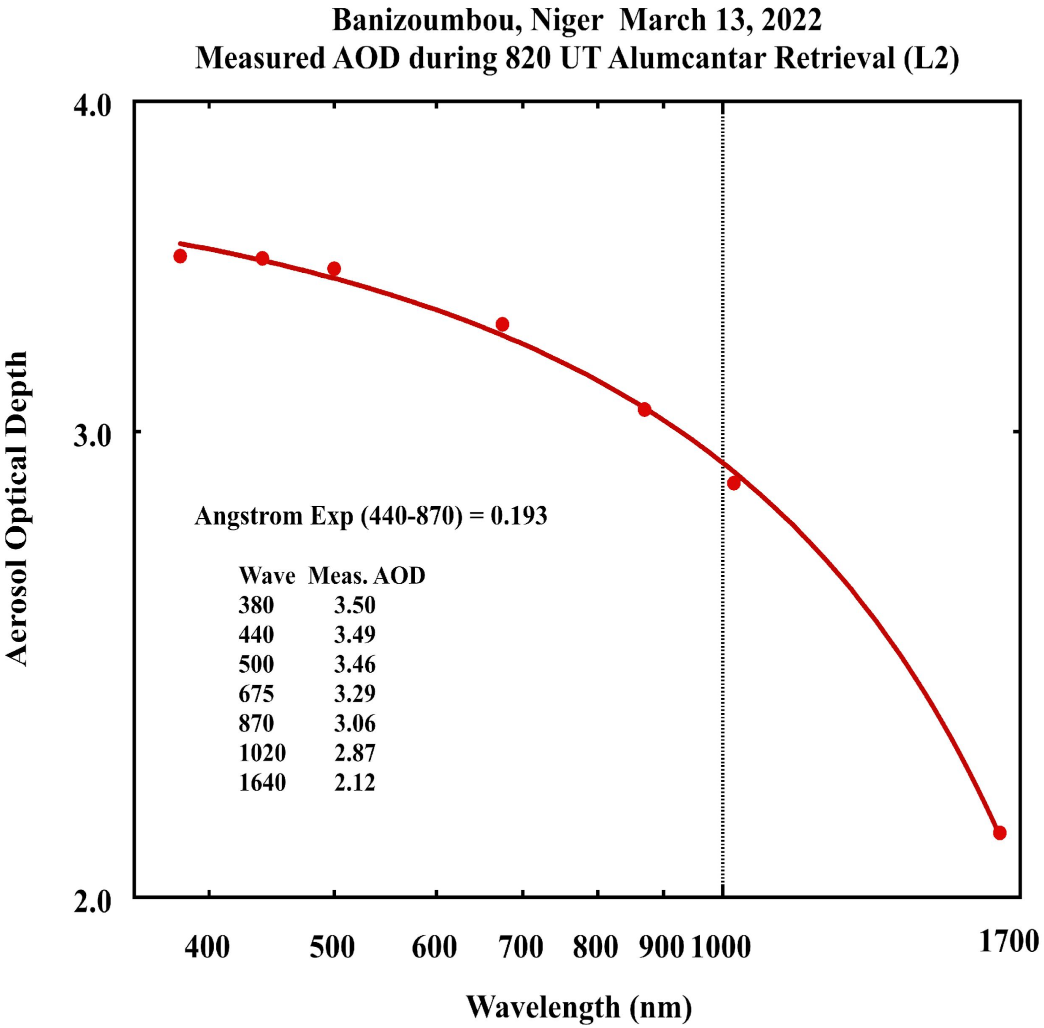

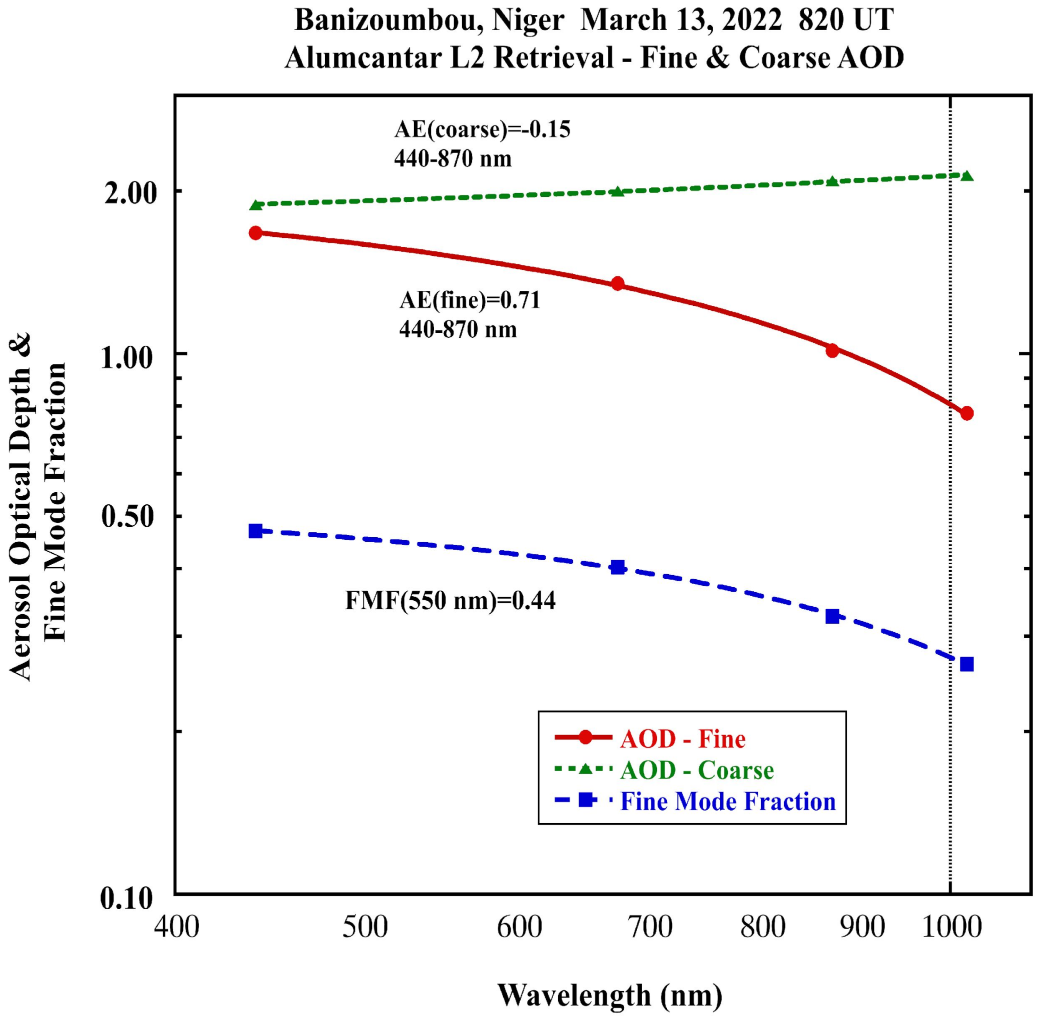

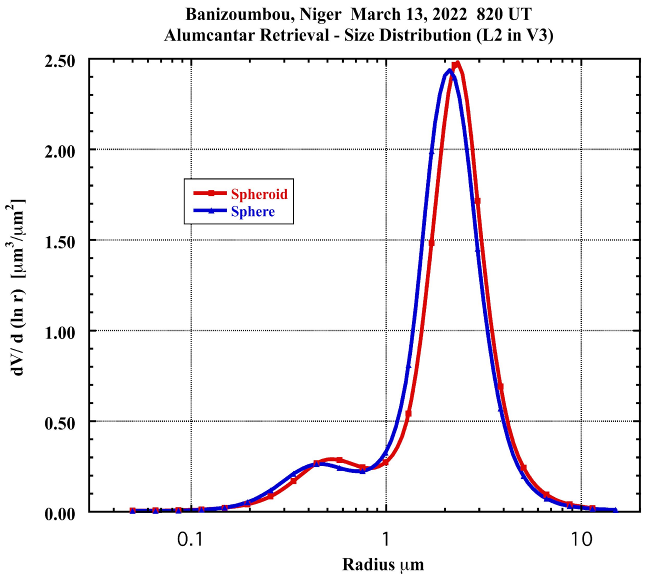

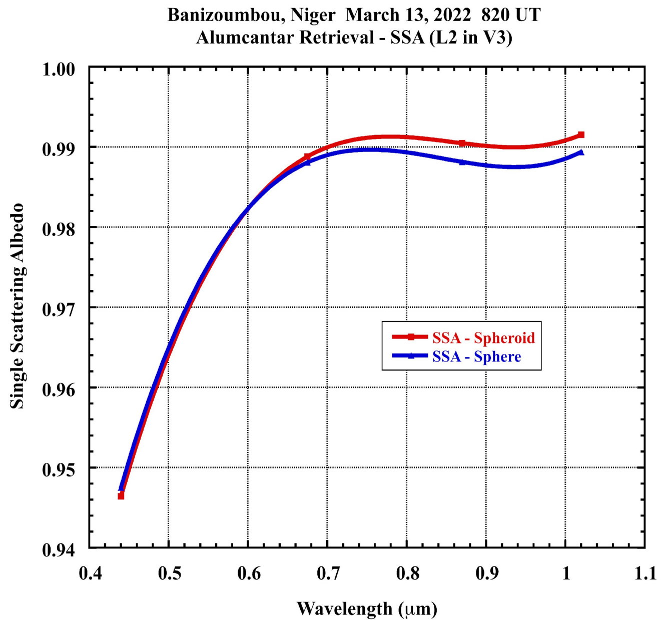

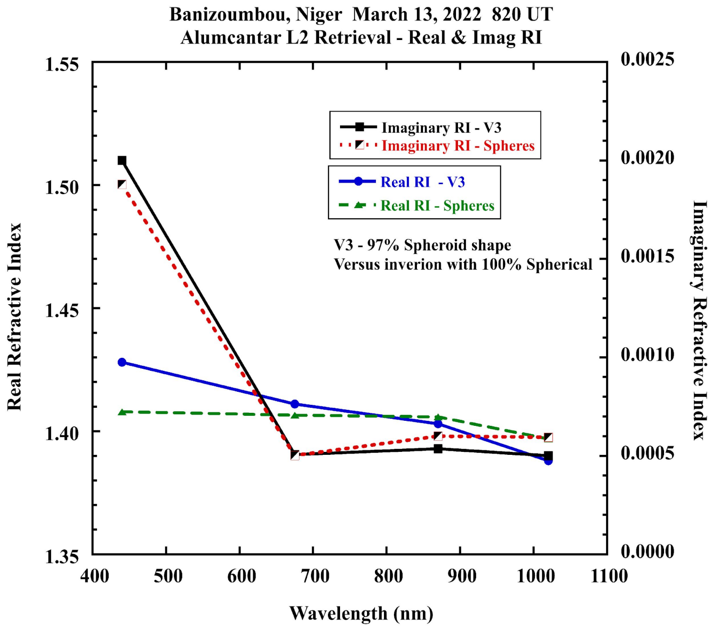

Banizoumbou, Niger Mar 13, 2022
AOD(440)=3.49 AE=0.195

V3 L2 Almucantar retrieval with 97% Spheroidal particle shape versus retrieval made with 100% Spherical particle shape

Relatively similar retrievals for the two different particle shape assumptions; especially for SSA
Very High AOD results in multiple scattering which likely reduces the effect of particle shape for this case.

Both cases have very low AE yet the Dakar case has a much broader coarse mode with a shoulder of significant 'middle mode' sized particles

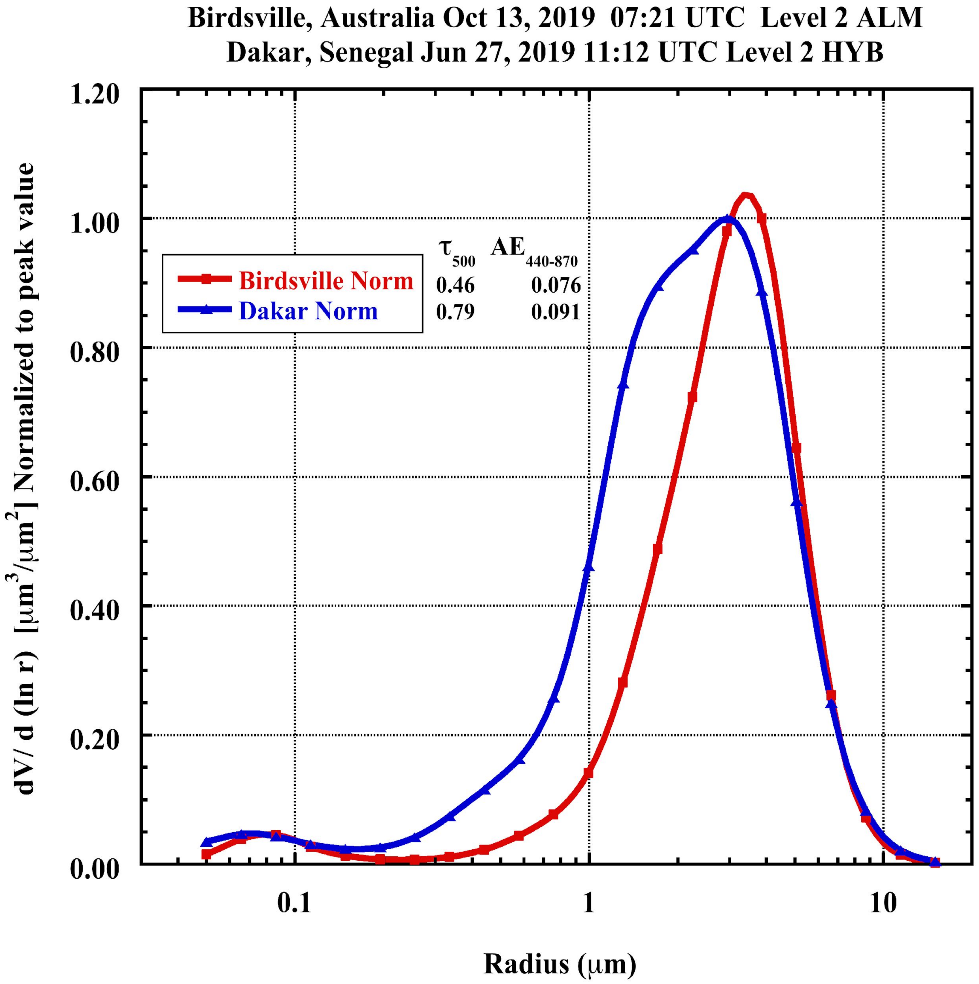

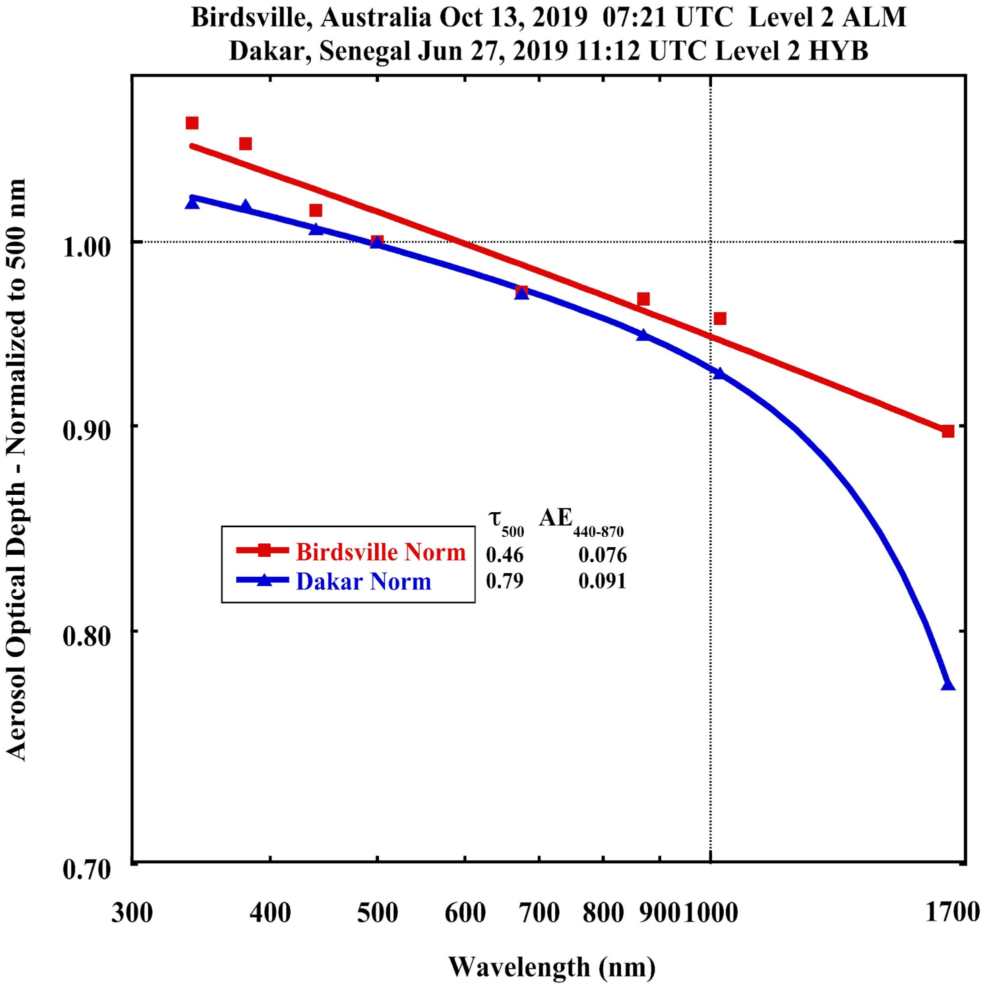

The AOD spectra is linear in log space (Angstrom fit) for the Birdsville case (minimal middle mode), with all wavelengths including 1640 nm fit to less than 0.01 in AOD. Note that this is unusual for dust cases since the vast majority have significant middle mode sized particles.

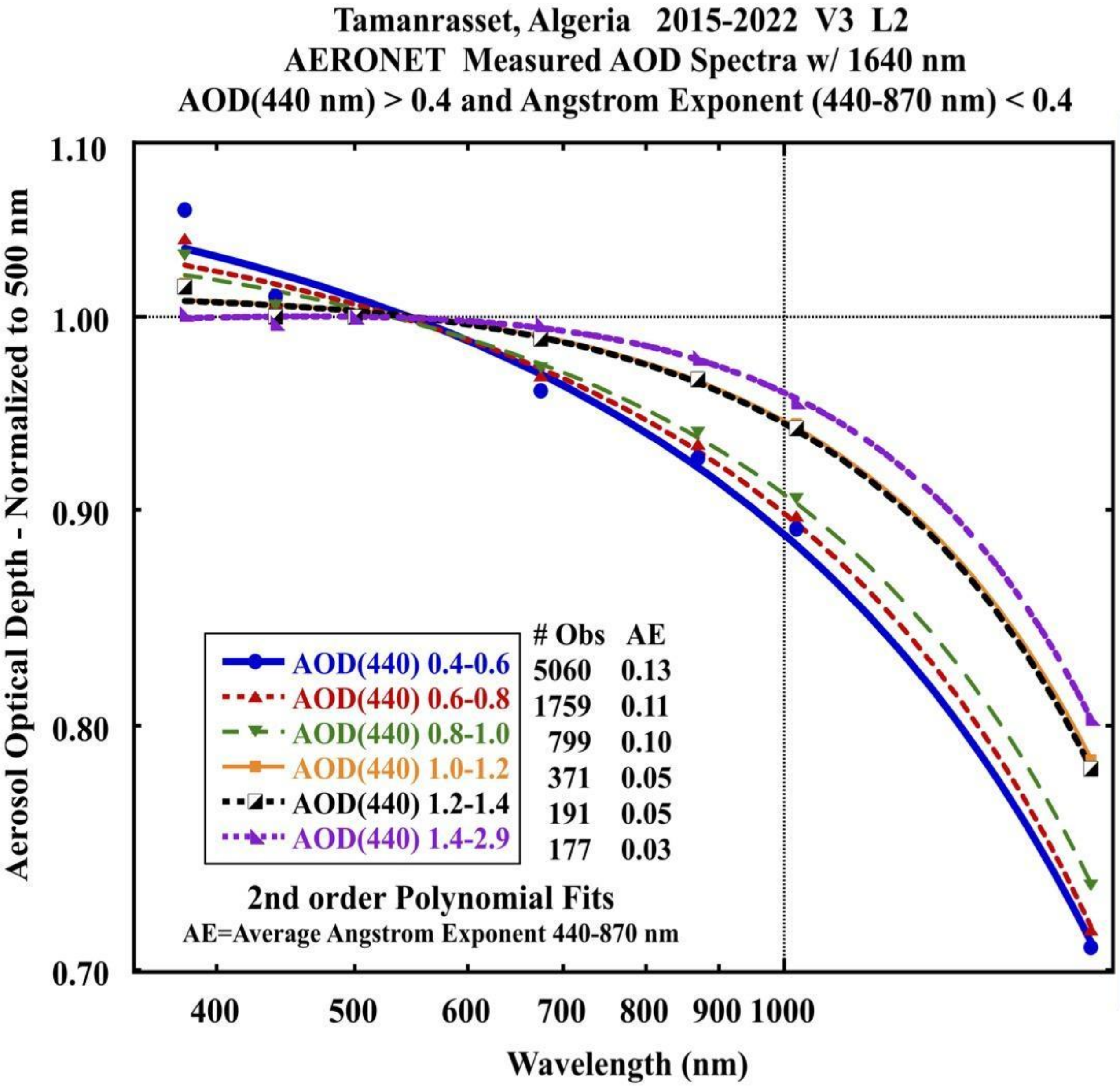

All instantaneous Level 2 AOD spectra (8357 obs.) from 2015-2022 averaged in AOD range bins.

2nd order polynomials (**in linear coordinates however**) fit the averaged AOD spectra well from 380 to 1640 nm, within the AERONET AOD measurement uncertainty of 0.01-0.02 (higher in the UV).

Note the significant decrease in AOD at 1640 nm relative to 870 and 1020 nm. This is consistent with the "middle mode" sized particles (~0.33-0.76 µm radius) which have a relatively small Angstrom Exponent (AE) in the visible to 870 nm but larger AE at longer wavelengths.

Summary and Conclusions

- Single Scattering Albedo – Close agreement between Di Biagio lab measurements of soil samples for Saharan and Sahelian sites plus a Middle Eastern site (Saudi Arabian peninsula). The 2 standard deviation tails of Sahel/Saharan site data (both highest and lowest 2% of values) also agree well (within ~0.01-0.02) to the least absorbing soil samples (Bodele Depression) and most absorbing Sahel samples (Mali and Niger).

- Single scattering Albedo – seasonal cycle at some Sahelian/Saharan sites (Ilorin & Dakar) with a minimum to maximum range in SSA of ~0.04 at 440 nm. Possibly due to seasonal shift in advection from various dust source regions with varying iron oxide contents.

- Size Distribution – Sahelian/Saharan sites all show persistent middle mode (radius ~0.33 to 0.76 micron) for all seasons. The middle mode also exists for the single sites in Australia, Saudi Arabia, and Mongolia but is not as pronounced as in the Sahara/Sahel region.

- Spectral AOD – The middle mode sized particles are consistent with the relatively large decrease in AOD at 1640 nm measured for most dust site data with low AE values